Reviewed Preprint
v1 • June 22, 2026
Not revised

For correspondence:
jczp@sri.utoronto.ca

Competing interests: No competing interests declared

Funding: See page 23

Reviewing editor: Sarah Russell, Peter MacCallum Cancer Centre, Australia



# Uncovering the Heterogeneity and Ontogeny of Mouse Thymic Macrophages Reveals an Unexpected Early Checkpoint Role

**Helen Wang[1,2], Vinothkumar Rajan[1,2], Anthony Wong[1,3], Slava Epelman[1,3,4,5], Juan Carlos Zúñiga-Pflücker[1,2]**

[1]Department of Immunology, University of Toronto, Toronto, Canada • [2]Biological Sciences, Sunnybrook Research Institute, Toronto, Canada • [3]Toronto General Hospital Research Institute, University Health Network, Toronto, Canada • [4]Ted Rogers Centre for Heart Research, Translational Biology and Engineering Program, Toronto, Canada • [5]Peter Munk Cardiac Centre, University Health Network, Toronto, Canada

## eLife Assessment

This study characterizes the heterogeneity and developmental origins of macrophages in the thymus and offers tantalizing evidence of their potential involvement in the first step of T cell selection. The macrophage characterisation is interesting, although the evidence for the specific involvement of macrophages in beta-selection is **incomplete**, as alternative explanations have not been ruled out. These results provide an **important** advance that further our understanding of thymus biology, especially in view of the contribution of heterogenous thymic macrophage subpopulations.

https://doi.org/10.7554/eLife.109219.1.sa2

## Abstract

Thymic macrophages (TMs) are critical for maintaining thymus homeostasis, yet their heterogeneity and specific functions in T cell development remain unclear. Through single-cell RNA sequencing and transgenic reporter mice, we revealed two novel TM subsets characterized by distinct surface markers and transcriptional programs. TIMD4$^+$ VCAM1$^+$ CX3CR1$^-$ TMs were enriched for phagocytic and apoptotic-cell–clearance pathways, whereas TIMD4$^-$ VCAM1$^+$ CX3CR1$^+$ TMs exhibited elevated expression of antigen-presentation machinery and interferon-response genes. Pseudotime trajectory analysis indicated a potential lineage progression from TIMD4$^-$ VCAM1$^+$ CX3CR1$^+$ precursors toward TIMD4$^+$ VCAM1$^+$ CX3CR1$^-$ effectors. Functional interrogation using fetal thymic organ cultures and the MaFIA depletion mouse model demonstrated that acute loss of TMs severely impaired thymocyte development, particularly at the pre-T cell receptor (TCR) β-selection checkpoint. TM ablation led to marked reductions in post-β-selection thymocyte subsets, implicating TMs in both survival and differentiation signals required for early T cell development. Mechanistically, TM depletion disrupted pre-TCR signaling and hindered transition through β-selection, likely due to absence of both apoptotic-cell clearance and differentiation cues provided by specialized TM subsets. These findings define two distinct TM populations and establish their role in orchestrating thymocyte maturation. By elucidating TM subset specialization and their dynamic contributions to the β-selection process, our findings advance our understanding of thymic microenvironment interactions and highlights macrophage heterogeneity as a key regulator of T cell development.

## Introduction

The thymus is the primary lymphoid organ dedicated to the generation of a diverse and self-tolerant repertoire of T lymphocytes, a process fundamental to adaptive immunity (1). This intricate T cell developmental program unfolds within a highly organized microenvironment composed of thymic epithelial cells (TECs), endothelial cells, and various hematopoietic populations, which collectively provide the essential signals for thymocyte differentiation, proliferation, and selection (2–4). The developmental journey of a T cell begins when bone marrow-derived thymic seeding progenitors (TSPs) enter the thymus at the cortico-medullary junction (CMJ) and commit to the T cell lineage, initiating a multi-stage differentiation cascade (5–7).

This journey is punctuated by a series of stringent checkpoints that assess the integrity and functionality of the nascent T cell receptor (TCR) repertoire (8,9). The earliest stages occur in the thymic cortex, where progenitors, lacking expression of CD4 and CD8, termed double-negative (DN) thymocytes (6), start to differentiate, which is characterized by the expression of CD44 and CD25 (3,4). Progression from the DN1 ($CD44^+CD25^-$) to the DN2 ($CD44^+CD25^+$) and DN3 ($CD44^-CD25^+$) stages is marked by the initiation of V(D)J recombination at the *Tcrb*, *Tcrg*, and *Tcrd* gene loci (1). The DN3 stage represents the first critical checkpoint in αβ T cell development, known as β-selection (12,13). Here, thymocytes that have successfully rearranged a functional TCRβ chain pair it with the invariant pre-TCRα chain (pTα) to form the pre-TCR complex. Successful signaling through this complex provides vital survival, proliferation, and differentiation cues, allowing the cell to progress to the DN4 stage and subsequently to the $CD4^+CD8^+$ double-positive (DP) stage (14,15). Thymocytes failing to generate a functional pre-TCR are eliminated via apoptosis, ensuring that only cells with a viable TCRβ chain continue their developmental progression (14).

Following β-selection, DP thymocytes undergo further TCRα chain rearrangement and are subjected to two additional selection events. Positive selection ensures that the fully assembled αβ TCR can recognize self-peptides presented by major histocompatibility complex (MHC) molecules on cortical (c)TECs, a process essential for TCR MHC-restriction (16–18). Subsequently, negative selection in the medulla eliminates thymocytes whose TCRs bind with high affinity to self-peptides presented by medullary (m)TECs and dendritic cells (DCs), thereby establishing central tolerance (19,20). These selection processes are notably stringent, resulting in the apoptotic death of over 95% of all developing thymocytes (21).

Integral to this journey and processes are thymic macrophages (TMs), which have long been recognized for their critical homeostatic function. Residing in both the cortex and medulla, TMs are exceptionally efficient phagocytes, responsible for the swift and silent clearance of the millions of apoptotic thymocytes generated daily (22–25). This process, known as efferocytosis, is vital for preventing the release of potentially immunogenic and inflammatory intracellular contents and maintaining the integrity of the thymic architecture (26). However, this view of TMs as mere "housekeepers" is rapidly evolving. Recent advances, particularly single-cell RNA sequencing (scRNA-seq), have revealed significant heterogeneity within the TM compartment, suggesting functional specialization (27). Two principal subsets have been identified in the adult mouse thymus: cortical TIMD4+ macrophages, which have potent efferocytosis function, and CX3CR1+ macrophages, which are enriched at the CMJ and express genes associated with antigen presentation, suggesting at a potential role in negative selection (27).

Despite these advances, our understanding of the full spectrum of TM function remains incomplete. While a role in clearing the cellular debris from positive and negative selection is well-established, and a contribution to negative selection itself is hypothesized, the involvement of TMs in the earliest stages of T cell development has been largely overlooked. The β-selection checkpoint, a nexus of proliferation, survival, and lineage commitment, occurs in a microenvironment rich in TMs. Yet, whether these macrophages are passive bystanders or active participants in this critical decision-making process is unknown.

The objective of this study is to investigate the role of thymic macrophages in early T cell development, with a specific focus on the β-selection checkpoint. By integrating high-resolution transcriptomic analysis, fate-mapping models, and functional assays, we sought to dissect the interactions between distinct TM subsets and developing DN thymocytes. Our findings reveal a previously unappreciated function for thymic macrophages in actively shaping the outcome of β-selection, thereby influencing the survival and differentiation of early T cell precursors. This work redefines the role of thymic macrophages, expanding their function beyond efferocytosis to include direct participation in the foundational checkpoints of T cell repertoire formation.

# Materials and methods

## Animals

Macrophage Fas-Induced Apoptosis (MaFIA), *MafB*-mCherry-Cre, *Spic*$^{-/-}$, and C57BL/6J mice were purchased from the Jackson Laboratory. The *Flt3*-Cre × *Rosa*-mTmG mice and *Flt3*-Cre × *Rosa*-mTmG mice in the *Ccr2*$^{-/-}$ background were kindly provided by Dr. Slava Epelman (University Health Network, University of Toronto) (28). All animals were bred and maintained in specific pathogen-free conditions at the Comparative Research Facility of the Sunnybrook Research Institute (SRI). All animal procedures were approved by the Sunnybrook Health Sciences Centre Animal Care Committee (Toronto, Ontario, Canada).

## Timed pregnancies and embryonic thymus analysis

Timed pregnancies were set up by housing male mice (8–24 weeks of age) in separate cages and mating them with female mice (8–24 weeks of age) overnight. The following morning, females were separated from the males, and successful matings were identified by the presence of a vaginal plug. The gestational age of the embryos was designated as embryonic day 0.5 (E0.5) on the day the plug was observed. Thymuses were harvested from embryos at E15 and E17, as well as from postnatal mice at 1 day, 1 week, and 3 weeks of age, in addition to adult (6-8 weeks) mice. Following collection, thymuses were subjected to enzymatic digestion to dissociate the tissue into single-cell suspensions. The resulting cells were stained for flow cytometric analysis.

## Intravenous CD45 staining

A CD45-Phycoerythrin (PE) antibody (30-F11; BioLegend) was diluted in phosphate buffered saline (PBS) to a final concentration of 1.5 μg/150 μL. The antibody solution was administered via tail vein injection using a 1 mL insulin syringe. Three minutes after the injection, mice were euthanized, and thymuses were harvested. The collected tissue was then processed and stained for flow cytometric analysis.

## Cell isolation from thymus

Thymocytes were harvested and subjected to enzymatic digestion using the Spleen Dissociation Kit (Miltenyi Biotec) and the gentleMACS™ Dissociator (Miltenyi Biotec) according to the manufacturer's instructions. The resulting cell suspensions were filtered through a 70 μm cell strainer to remove debris, resuspended in PBS, and kept on ice until further processing.

## Flow cytometry

Single-cell suspensions ($1 \times 10^7$ cells) were prepared from the thymus and stained in a 96-well conical bottom plate (ThermoFisher Scientific). The staining cocktail included the fixable viability dye eFluor 450 (eBioscience), diluted 1:800 in PBS, anti-CD16/32 to block Fc receptors, and the desired fluorochrome-conjugated antibodies targeting macrophages and T cells (see **Supplemental Tables 1 and 2** for details). Cells were initially stained with eFluor 450 in PBS for 15 minutes on ice. After washing with fluorescence-activated cell sorting (FACS) buffer, anti-CD64, anti-CCR2, and anti-VCAM1 antibodies were added to the wells, and cells were stained for an

additional 15 minutes on ice. To block non-specific binding, Fc-block antibody was added to the cells 15 minutes prior to the addition of the remaining antibody cocktail, which was incubated with the cells for 30 minutes on ice.

Following staining, cells were washed and resuspended in FACS buffer for flow cytometric acquisition using the FACSymphony™ A5 Cell Analyzer (BD Biosciences). Data were analyzed with FlowJo software (TreeStar). The complete list of antibodies and their corresponding clones is provided in Supplemental Tables 1 and 2.

## Cell sorting

Thymuses were harvested from 6-week-old C57BL/6 mice and subjected to enzymatic digestion using the Spleen Dissociation Kit (Miltenyi Biotec) and the gentleMACS™ Dissociator (Miltenyi Biotec) to generate single-cell suspensions. After cell isolation, cells were counted and stained with allophycocyanin (APC)-conjugated anti-mouse CD64 antibody in FACS buffer for 20 minutes on ice (see Supplemental Table 1 for antibody details). Following a wash with FACS buffer, cells were stained with anti-APC MicroBeads (Miltenyi Biotec) for 20 minutes on ice. The cells were then washed again with FACS buffer and loaded onto LS columns (Miltenyi Biotec) for positive selection of $CD64^+$ cells. After selection, the cells were washed and further stained with antibodies against F4/80, TIMD4, Ly6C, and CD45 for 30 minutes on ice (see Supplemental Table 1 for antibody details). The stained cells were sorted using the FACSAria™ Fusion Flow Cytometer (BD Biosciences). $CD64^+$ sorted cells were collected in 1.5 mL Eppendorf tubes containing 300 µL of FBS, counted, and resuspended in PBS supplemented with 0.04% BSA. Cells were then encapsulated, and library preparation was performed using the Chromium Single Cell 3' Reagent Kit (10X Genomics). Gene expression libraries were sequenced on a NovaSeq 6000 platform (Illumina) at Azenta Life Sciences. In total, 3,214 and 2,815 cells were sequenced from two independent experiments.

## Fetal thymus organ culture (FTOC) and TM depletion in MaFIA mice

Timed pregnancies were set up for MaFIA mice as described above. Fetal thymuses were harvested at E15.5 for FTOC. Briefly, culture wells were set up in a 12-well-plate 24 hour before FTOC. In each well, Whatman® Nuclepore™ Track-Etched membrane (WHA110409; Sigma) was placed on top of SURGIFORM® absorbable gelatin sponge (1974; Ethicon) in 1.5 mL of complete Dulbecco's Modified Eagle Medium (DMEM) (supplemented with 10% Fetal Bovine Serum, 2 mM L-glutamine, 100 U/mL penicillin and 100 µg/mL streptomycin) (29,30). Three fetal thymuses were placed on top of the membrane for each well. B/B homodimerizer stock was diluted to 2.5 µM in complete DMEM and added to the thymus lobes at the time of culture setup and again on the following day. On day 2, the membrane with the thymus lobes was transferred to a fresh culture plate containing new gelatin sponge and complete DMEM. Cultures were maintained in 37 °C incubator until day 6, at which point the thymic lobes were processed for flow cytometry analysis as described above.

## Transcriptomic analysis

$CD64^+$ cells were isolated from the thymus of C57BL/6J adult mice and processed for scRNA-seq as described below. Data from each scRNA-seq experiment underwent pre-processing as detailed below. Quality control filters were applied to remove cells with more than 12.5% mitochondrial gene expression, fewer than 500 reads, or more than 6,000 reads, ensuring the retention of high-quality cells for analysis. Macrophages and monocytes were identified using a module scoring approach, and their respective cell barcodes were recorded. These barcodes were used for subsetting before merging the datasets from the two scRNA-seq experiments with published TM data from Dzhagalov's group. The merging was performed using Harmony to align the datasets and correct for batch effects. Following integration, cells were clustered, and module scores were assigned to all identified clusters. Non-relevant cell types, including B cells, T cells, and DCs, were excluded from subsequent analyses to focus on macrophages and monocytes.

## Analysis of scRNA-Seq and data integration

All analyses were performed using R software version 4.4.1. Cells expressing fewer than 500 genes or more than 6,000 genes were excluded from the dataset. Additionally, cells with greater than 12.5% mitochondrial gene content were removed to ensure data quality. The dimensionality of the dataset was assessed using an Elbow plot to determine the appropriate number of principal components. Gene ontology (GO) enrichment analysis of differentially expressed genes (DEGs) was conducted to identify overrepresented biological processes using the FindMarkers function from the Seurat package (31). The data were then integrated with previously published scRNA-seq datasets on TMs (GEO: GSE185460), as well as datasets from heart, liver, and lung macrophages (GEO: GSE188647), from the laboratories of Drs. Dzhagalov and Epelman, respectively. Batch correction across datasets was performed using the Harmony package (27,32,33). Following integration, the merged dataset was normalized using the SCTransform method to account for technical variation. For data visualization, Uniform Manifold Approximation and Projection (UMAP) was applied to reduce dimensionality and enable visualization of cellular clustering patterns.

## Trajectory analysis using Monocle3

Trajectory analysis was performed using Monocle3 to infer the developmental trajectory of TMs (34). Prior to this, TM datasets were normalized and integrated using the SCTransform method implemented in Seurat. From the resulting Seurat object, the expression matrix, cell metadata, and gene metadata were extracted to construct a CellDataSet (CDS) object, which serves as the foundational data structure in Monocle3. Pre-processing steps were applied to the CDS to ensure high-quality trajectory inference. Principal component analysis (PCA) was first conducted to reduce dimensionality while preserving variance across the dataset. This was followed by non-linear dimensionality reduction using Uniform Manifold Approximation and Projection (UMAP) to visualize the global structure of the dataset in a low-dimensional space. The cells were then re-clustered within Monocle3 to refine group assignments, ensuring that clusters corresponded accurately to biological populations. Trajectory inference was performed with the root node manually assigned to monocytes (defined by *Ly6c2* and *Ccr2* expression), reflecting their position as the presumptive progenitor population in the trajectory.

## Statistical analysis

Data are presented as the mean ± standard error of the mean (SEM). Univariate comparisons between two groups were performed using the Mann-Whitney U test. For analyses involving more than two groups, the normality of the data was assessed using the D'Agostino-Pearson test and/or inspection of Q-Q plots, while homoscedasticity (equal variance) was evaluated using the Brown-Forsythe test or by examining residual plots. Non-parametric comparisons across multiple groups were conducted using the Kruskal-Wallis test, followed by post-hoc pairwise comparisons of the mean ranks of each group with the mean rank of the control group. Multiple comparisons were adjusted using Dunn's test to control for type I error. For pairwise comparisons involving more than two groups, the Holm-Šídák method was applied to correct for multiple comparisons, reducing the likelihood of type I error. All statistical analyses were performed using GraphPad Prism version 10.

# Results

## Identification of Two Distinct Tissue-Resident Macrophage Subsets in the Adult Thymus

To investigate the heterogeneity of phagocytic cells within the thymus, we performed multi-parameter flow cytometry on hematopoietic cells ($CD45^+$) from the thymus of adult mice. We first identified the total TM population based on the co-expression of the canonical markers CD64 and

F4/80 (Figure 1A-B). The majority of these CD64$^+$ F4/80$^+$ cells also expressed the phagocytic receptor MerTK, consistent with their identity as macrophages (35).

To resolve heterogeneity within this population, we further analyzed for the expression of TIMD4 and VCAM1. This revealed three distinct subsets within the CD64$^+$ F4/80$^+$ gate: a major TIMD4$^+$ VCAM1$^+$ population, a smaller TIMD4$^-$ VCAM1$^+$ population, and a minor TIMD4$^-$VCAM1$^-$ population (Figure 1C-E). To clarify the identity of these subsets, we utilized MafB-mCherry and Csf1r-EGFP reporter mice. Both the TIMD4$^+$ VCAM1$^+$ and TIMD4$^-$ VCAM1$^+$ subsets expressed high levels of MafB (mCherry$^+$), a transcription factor crucial for mature tissue-resident macrophages (TRMs), while the TIMD4$^-$ VCAM1$^-$ subset was MafB-negative and expressed high levels of CSF1R (GFP$^+$), a marker associated with monocytes (Figure 1F).

To definitively distinguish these thymus resident populations from circulating cells and further define their identity, we performed intravenous (IV) labeling with an anti-CD45 antibody. Both the TIMD4$^+$ VCAM1$^+$ and TIMD4$^-$ VCAM1$^+$ macrophage populations were largely protected from IV labeling (CD45$^-$), confirming their parenchymal, tissue-resident localization (Figure 2A, B, C). Furthermore, these two subsets lacked expression of classical monocyte-associated markers, including Ly6C, CCR2, and CX3CR1 (Figure 2D, E). In contrast, the TIMD4$^-$ VCAM1$^-$ subset expressed high levels of these monocyte markers, confirming its identity as a population of thymic monocytes rather than mature macrophages.

Taken together, our analysis robustly identifies two distinct subsets of *bona fide* tissue-resident thymic macrophages, a dominant TIMD4$^+$ VCAM1$^+$ population and a TIMD4$^-$ VCAM1$^+$ population, alongside a separate population of thymic monocytes. This phenotypic framework allows for the specific investigation of the functional roles of each macrophage subset in thymic biology.

## Transcriptomic Profiling by scRNA-seq Confirms Two Functionally Distinct Macrophage Subsets

To gain deeper insight into the transcriptional identities of these macrophage populations, we performed scRNA-seq on sorted thymic CD45$^+$ CD64$^+$ cells. Unbiased clustering of the resulting 3,153 cells revealed five distinct myeloid clusters, including monocytes, proliferating macrophages, and two major quiescent macrophage populations that corresponded directly to our flow cytometry findings (Figure 3A).

A major macrophage cluster was defined by high expression of *Timd4*, *Vcam1*, *Mertk*, and the transcription factor *Maf*, confirming its identity as the TIMD4$^+$ VCAM1$^+$ population (Figure 3B). In contrast, the other major macrophage cluster was defined by high expression of *Vcam1* and *Cx3cr1*, aligning it with the TIMD4$^-$ VCAM1$^+$ subset (Table 1), as identified above. Intriguingly, the TIMD4$^+$ VCAM1$^+$ CX3CR1$^-$ cluster also showed uniquely high expression of *Spic*, the lineage-defining transcription factor for splenic red pulp macrophages (RPMs) (36). To test for a shared developmental dependency, we analyzed SpiC knockout (*Spic*$^{-/-}$) mice. While *Spic*$^{-/-}$ mice exhibited the expected loss of RPMs, the numbers of both thymic macrophage subsets were unaltered, suggesting that TMs utilize a Spic-independent developmental pathway despite their transcriptional similarities (Figure 3C).

To formally assess the functional specialization suggested by these transcriptional profiles, we performed Gene Ontology (GO) pathway analysis. This revealed a stark functional dichotomy between the two subsets. The TIMD4$^-$ VCAM1$^+$ CX3CR1$^+$ TMs were significantly enriched for pathways related to "antigen processing and presentation via MHC class I" and "interferon signaling" consistent with their high expression of *H2-K1*, *H2-D1*, and *Runx3* and suggesting a role in T cell education (Figure 4A). Conversely, the TIMD4$^+$ VCAM1$^+$ CX3CR1$^-$ TM cluster was dominated by pathways associated with "phagocytosis" and "endocytosis," supporting a primary role in efferocytosis for apoptotic cell clearance (Figure 4B).

This functional role was confirmed by the identification of a sub-cluster within the TIMD4$^+$ VCAM1$^+$ CX3CR1$^-$ population that was actively engaged in efferocytosis *in vivo*. These cells co-expressed canonical T-cell transcripts such as *Cd3g* and *Trac* alongside their macrophage-specific

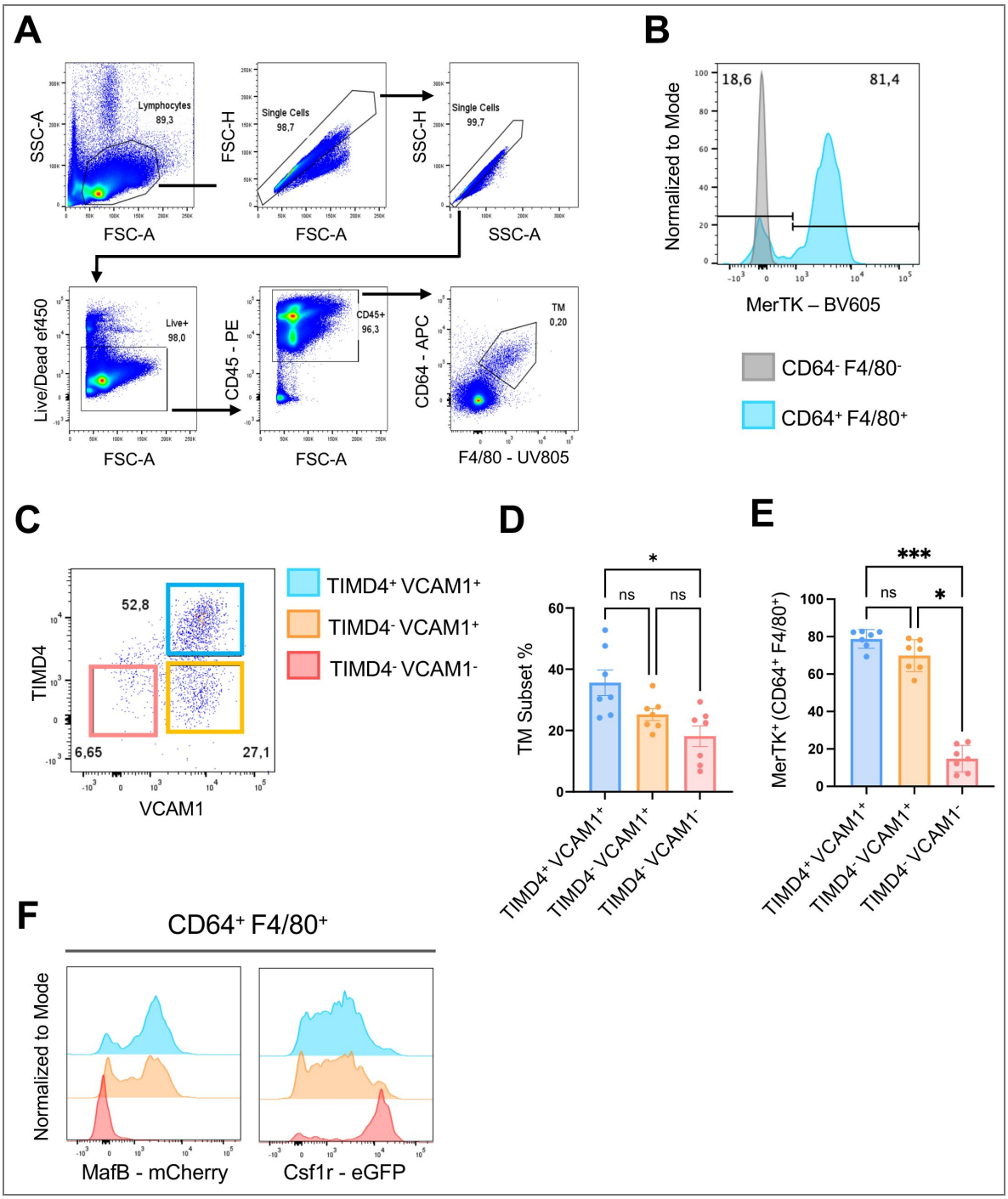


**Figure 1. TMs characterization using flow cytometry and immunofluorescent staining.**

Frozen thymic sections were used for immunofluorescent staining to identify the localization of TMs. Thymuses were harvested from C57BL/6 mice aged six to ten months and enzymatically digested for single-cell preparation. Cells were stained with antibodies for flow cytometric analysis. A) Gating strategy for identifying TMs. B) Representative flow cytometry histogram showing MerTK expression on TMs (blue) compared to $CD64^{-}F4/80^{-}$ lymphocytes (red). C) Identification of distinct TM subsets using TIMD4 and VCAM1 markers. D) Comparison of the percentages of TM subsets in six-month-old mice. E) Comparison of the percentages of $MerTK^{+}$ cells between TM subsets. F) Representative flow cytometry plots showing TM reporter expressions in *MafB*-mCherry and *Csf1r*-EGFP mice. Data are presented as the mean ± SEM (n = 7 per group from 2 independent experiments). A Kruskal-Wallis test was performed for multiple comparisons between three groups (*p ≤ 0.05).

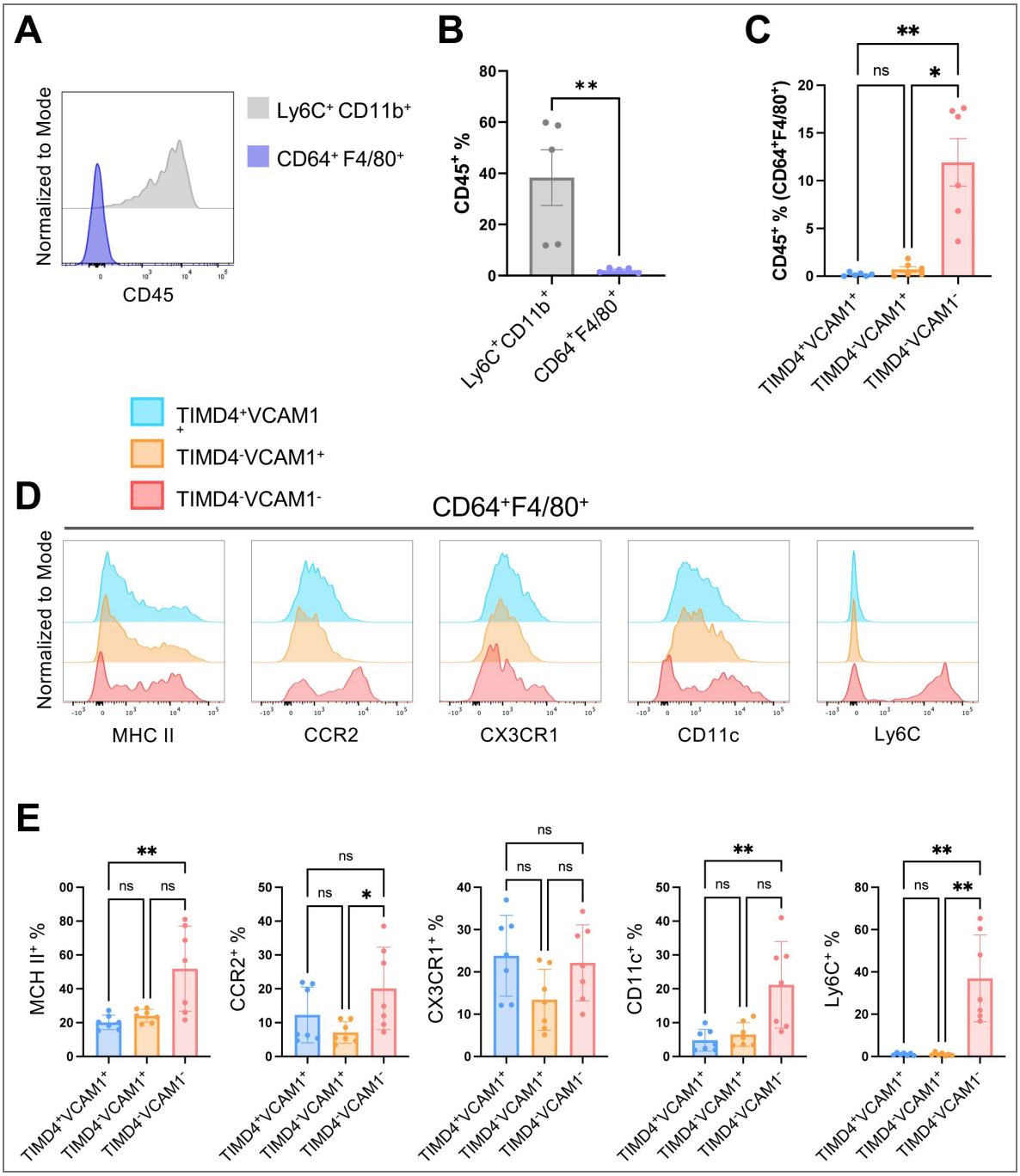


**Figure 2. Distinguishing TMs from thymic and circulating monocytes.**

Thymuses were harvested from six-month-old C57BL/6 mice and enzymatically digested for single-cell preparation. Cells were stained with antibodies for flow cytometric analysis. A) CD45 IV labeling of circulating leukocytes in the mouse thymus, distinguishing intravascular cells from thymic-resident populations. B) Comparison of the percentages of CD45 labeled cells between Ly6C$^+$CD11b$^+$ and CD64$^+$F4/80$^+$ cells in the thymus. C) Comparison of the percentages of CD45 labeled cells between TM subsets. D) Lack of expression of monocyte markers associated with TIMD4$^+$VCAM1$^+$ and TIMD4$^-$VCAM1$^+$ subsets. E) Comparative analysis of monocyte marker expression across TM subsets. Data are presented as mean ± SEM (n = 5-7 per group from 2 independent experiments). Statistical significance was assessed using a two-tailed Mann-Whitney test (**p ≤ 0.01) for comparisons between two groups. A Kruskal-Wallis test was performed for multiple comparisons between three groups (*p ≤ 0.05 and **p ≤ 0.01).

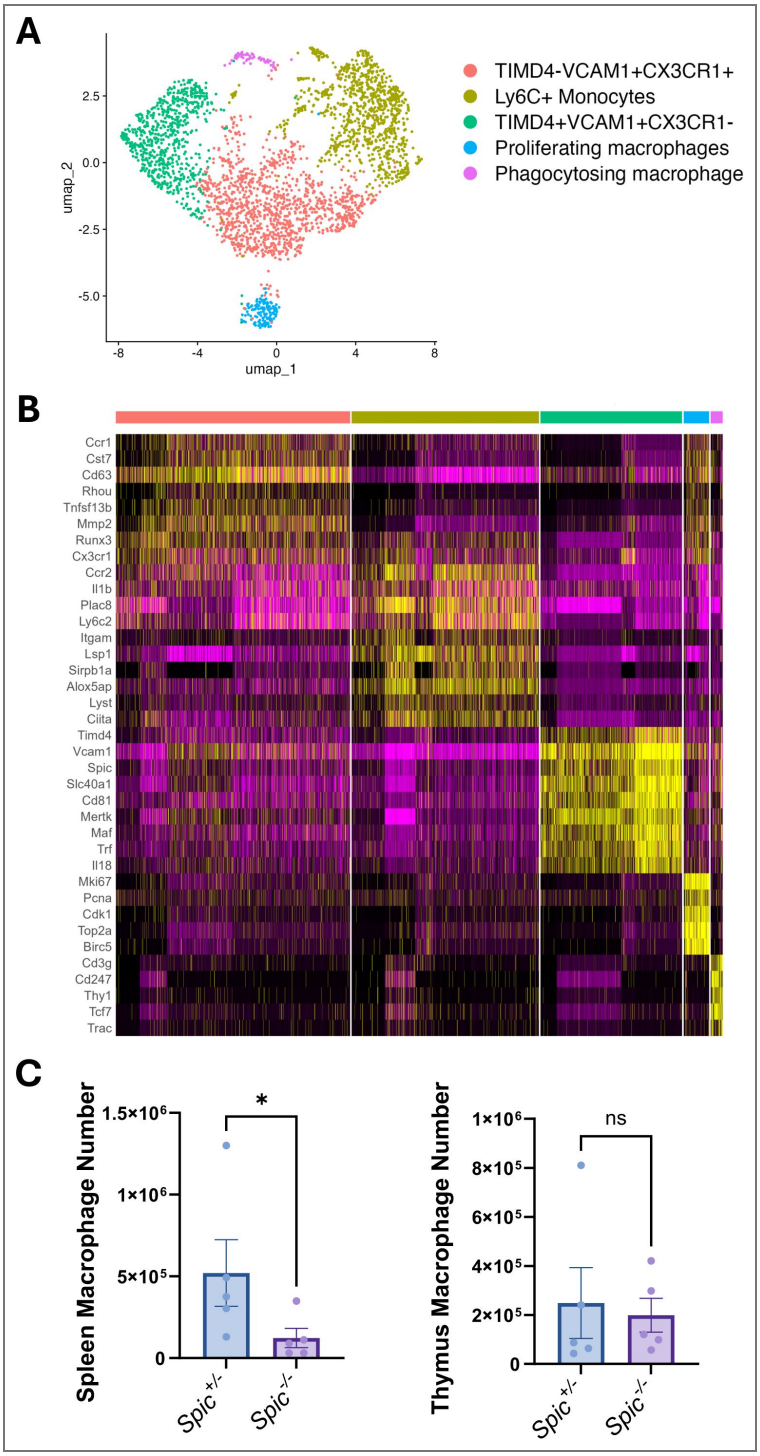


**Figure 3. Single-cell transcriptomics reveals distinct subpopulations and gene expression profiles of thymic macrophages.**

Thymuses were harvested from six-week-old C57BL/6 mice, and CD64⁺ cells were isolated by FACS for scRNA-seq using the 10x Genomics 3′ RNA-seq platform. For TM scRNA-seq, cells were pooled from six mice per sample, with each experiment performed independently in duplicate. The resulting dataset was integrated with published data from Dzhagalov's lab where they sequenced from Cd11cYFP and MaFIA mice using Harmony for batch correction and alignment. A) UMAP clustering of TMs. B) Heatmap representation of DEGs across the five clusters. C) Comparison of macrophage numbers in the thymus and spleen of *SpiC*$^{-/-}$ mice. Data are presented as mean ± SEM (n = 4-5 per group from 2 independent experiments), analyzed using a two-tailed Mann-Whitney test (*p ≤ 0.05).

| Ly6C$^+$ Monocytes | | TIMD4$^+$ VCAM1$^+$ CX3CR1$^-$ | | TIMD4$^-$ VCAM1$^+$ CX3CR1$^+$ | |
|---|---|---|---|---|---|
| *Lsp1* | *Ahnak* | *Cd163* | *Ccl2* | *Gpnmb* | *Lhfpl2* |
| *Sirpb1a* | *Cytip* | *Mrc1* | *Ccl4* | *Tnfsf13b* | *Chst2* |
| *Gm34084* | *Ifitm2* | *Mertk* | *Adgre1* | *Lhfpl2* | *Mmp2* |
| *Alcam* | *S100a11* | *Spic* | *Adgre2* | *Chst2* | *Pmepa1* |
| *Cbfa2t3* | *Ramp1* | *Timd4* | *Hmox1* | *Mmp2* | *Oas3* |
| *Sirpb1b* | *Lyst* | *Vcam1* | *Tlr7* | *Pmepa1* | *Cst7* |
| *Cnn2* | *Ccl6* | *Clec1b* | *Axl* | *Oasl1* | *Zmynd15* |
| *Samsn1* | *Itga4* | *Stab2* | *Fgr* | *Cst7* | *H2-Q7* |
| *Itgam* | *Il17ra* | *Fcgrt* | *Ccl8* | *Zmynd15* | *Ccr5* |
| *Alox5ap* | *Ccr2* | *Tgm2* | *Id2* | *H2-M2* | *H2-T22* |
| *Emb* | *Ly6c2* | *P2ry12* | *Sirpa* | *Sh3pxd2b* | *Bst2* |
| *Traf1* | *Il1b* | *Cd86* | *Runx1* | *Kctd14* | *Stat2* |
| *Dpp4* | *Batf3* | *Tlr4* | *Stat5b* | *Ifit1* | *Cebpa* |
| *S100a10* | *Rbpj* | *Il18* | *Cd84* | *Fam20c* | *Il1rn* |
| *Plac8* | | *Ptgs1* | *Mapk14* | *Cp* | *Cxcl16* |
| *Stap1* | | *Pparg* | | *Spsb1* | |
| *Sirpb1c* | | *Adamdec1* | | *Gpnmb* | |
| *Rnase6* | | *Cd38* | | *Tnfsf13b* | |

**Table 1. Differentially expressed genes (DEGs) from scRNA-seq analysis.**

List of DEGs with an average $\log_2$ fold change > 1 and an adjusted p-value < 0.01, ordered by adjusted $\log_2$ fold change.

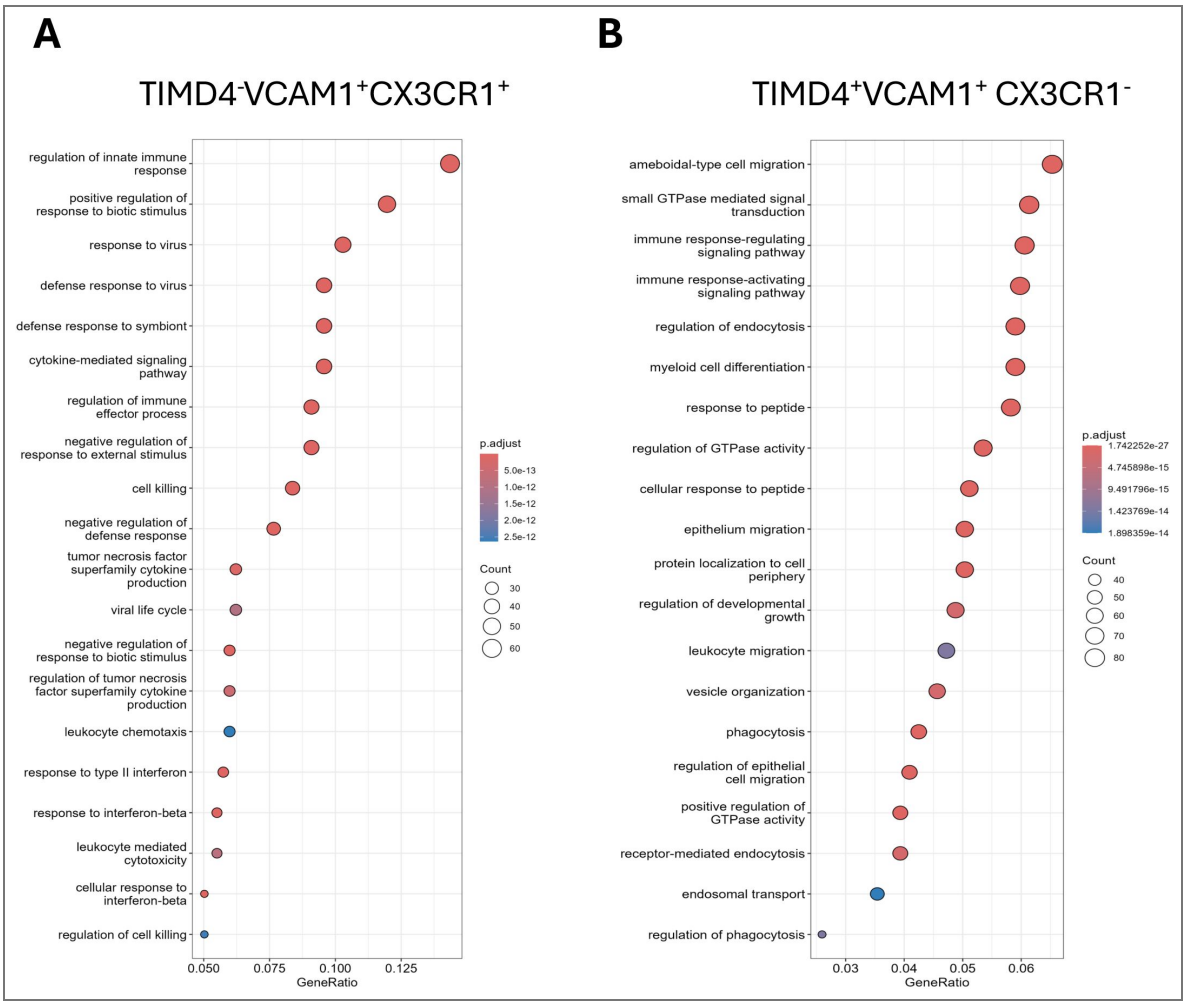


**Figure 4. GO pathway analysis of TMs.**

Thymuses were harvested from six-week-old C57BL/6 mice, and CD64$^+$ cells were isolated by FACS for scRNA-seq using the 10x Genomics 3′ RNA-seq platform. For TM scRNA-seq, cells were pooled from six mice per sample, with each experiment performed independently in duplicate. The resulting dataset was integrated with published data from Dzhagalov's laboratory where they sequenced from Cd11cYFP and MaFIA mice using Harmony for batch correction and alignment. A) Dotplot showing top 20 enriched GO pathways in TIMD4$^-$VCAM1$^+$CX3CR1$^+$ TM subset based on highly expressed genes. B) Dotplot showing top 20 enriched GO pathways in TIMD4$^+$VCAM1$^+$CX3CR1$^-$ TM subset based on highly expressed genes.

genes (Figure 3B). Thus, their T-cell transcriptional signature provides direct evidence of ongoing efferocytosis, capturing macrophages in the act of engulfing apoptotic thymocytes and confirming the potent phagocytic activity of TIMD4$^+$ VCAM1$^+$ CX3CR1$^-$ TMs.

## The Thymic Macrophage Compartment Undergoes Dynamic Remodeling During Development

To understand how the TM compartment evolves in parallel with the thymus itself, we analyzed the number and composition of TM subsets during ontogeny, from embryonic development through adulthood. Consistent with known thymic biology, the absolute number of total thymocytes and TMs peaked in young, 3-week-old mice, before declining with age, indicating that the size of the TM pool is coupled to the overall cellularity of the organ (Supplemental Figure 1A-B).

Further analysis of TM subset composition revealed a profound and dynamic remodeling process across the lifespan. At embryonic day 15 (E15), the nascent thymus was populated almost exclusively by macrophages with a progenitor-like phenotype (TIMD4$^-$ VCAM1$^-$), which co-expressed the monocyte-associated markers CD11b and CCR2 (Figure 5A). This suggests that the embryonic thymus is initially seeded by monocyte-derived precursors. Following birth, this landscape was dramatically reshaped. We observed a rapid postnatal expansion of the TIMD4$^+$ VCAM1$^+$ CX3CR1$^-$ subset, which became the major TM population in young mice, coinciding with the period of peak thymic size (Figure 5B). This indicates that the establishment of the mature, homeostatic TM pool is a key feature of postnatal thymic development. Interestingly, as mice aged and the thymus began to involute (6 weeks and older), the proportion of TIMD4$^+$ VCAM1$^+$ CX3CR1$^-$ macrophages steadily declined. This decline was accompanied by a progressive accumulation of the TIMD4$^-$ VCAM1$^+$ CX3CR1$^+$ TM subset, which became a more prominent feature of the aging thymus.

Together, these data reveal that the thymic macrophage compartment is not a static entity but is actively remodeled throughout life. Distinct TM subsets dominate at specific developmental windows, with an initial wave of progenitor-like cells being replaced by a homeostatic TIMD4$^+$ VCAM1$^+$ CX3CR1$^-$ population, which in turn gives way to a TIMD4$^-$ VCAM1$^+$ CX3CR1$^+$ population during the start of the thymic involution process.

## Thymic Macrophage Subsets Arise from Distinct Developmental Origins

Having established the dynamic nature of the TM compartment, we next sought to define the developmental origins of the two major macrophage subsets. We first utilized Flt3-Cre × Rosa-mTmG fate-mapping mice, in which cells passing through a FLT3-expressing hematopoietic stem cell (HSC)-derived progenitor stage are permanently labeled with GFP, while cells from an FLT3-independent pathway (i.e., yolk sac-derived) remain Tomato$^+$ (Figure 6A) (28). This fate-mapping analysis revealed a clear divergence in origin. The majority (>50%) of the homeostatic TIMD4$^+$ VCAM1$^+$ CX3CR1$^-$ macrophages were Tomato$^+$, indicating they arise from an FLT3-independent, likely embryonic/fetal, precursor and persist into adulthood (Figure 6B-C). In stark contrast, the vast majority of TIMD4$^-$ VCAM1$^+$ CX3CR1$^+$ TMs and thymic monocytes were GFP$^+$, demonstrating their origin from adult HSC-derived, FLT3-dependent progenitors.

Based on these findings, we hypothesized that the maintenance of the TIMD4$^-$ VCAM1$^+$ CX3CR1$^+$TM subset, but not the TIMD4$^+$ VCAM1$^+$ CX3CR1$^-$ subset, would depend on the continuous recruitment of CCR2-dependent monocytes from the bone marrow. To test this, we analyzed TM populations in *Ccr2* knockout (*Ccr2*$^{-/-}$) mice. While overall thymocyte numbers were unaffected, the composition of the TM compartment was significantly altered (Figure 7A). While there was no change in TIMD4$^+$ VCAM1$^+$ CX3CR1$^-$ macrophages number, the TIMD4$^-$ VCAM1$^+$ CX3CR1$^+$macrophage population and thymic monocytes was significantly decreased in *Ccr2*$^{-/-}$ mice (Figure 7B-D).

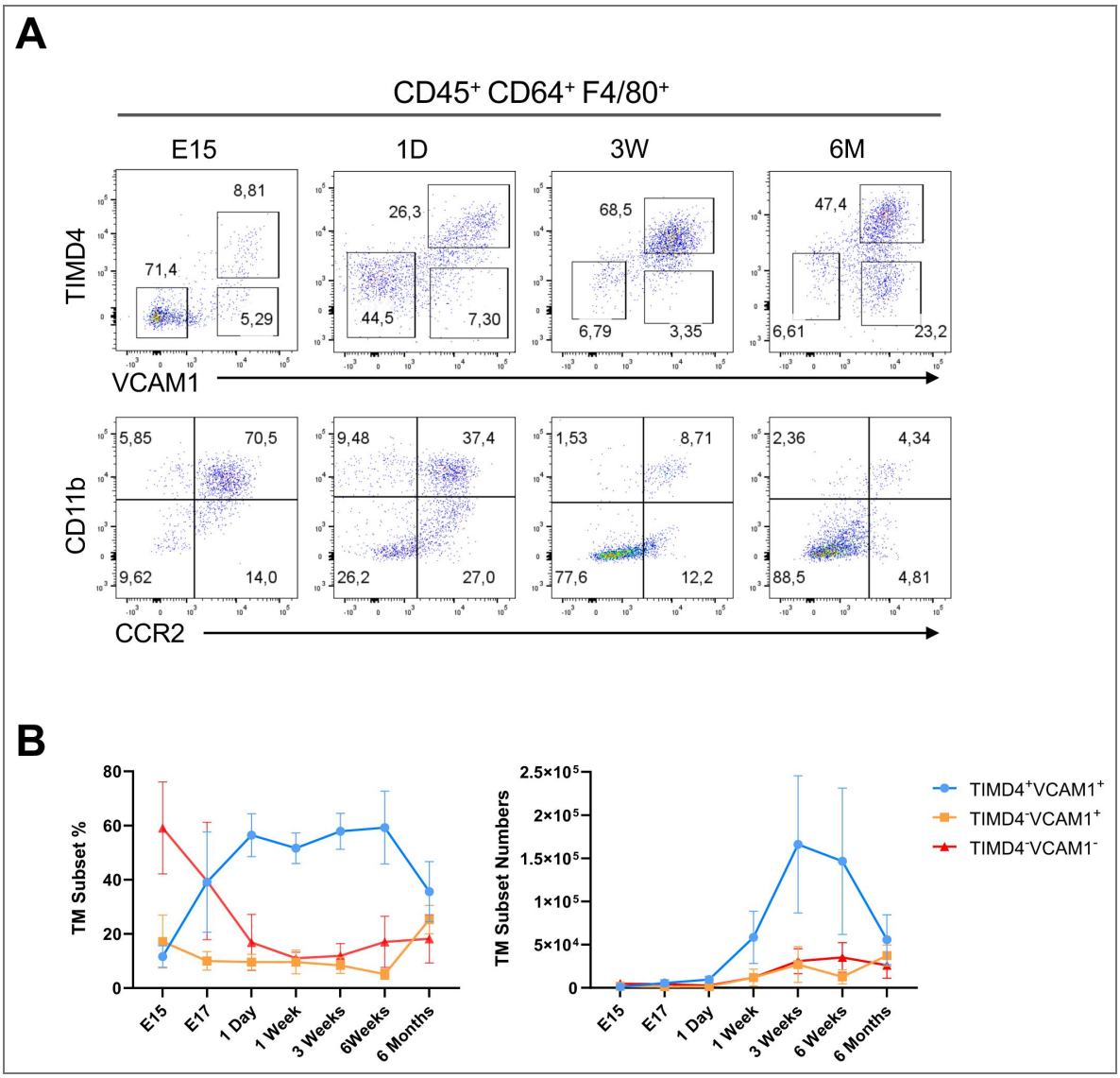


**Figure 5. Developmental progression of TM subsets.**

Thymuses were harvested from mice at various developmental time points and enzymatically digested to prepare single-cell suspensions. Cells were stained with antibodies for flow cytometry analysis. A) Expression of TM markers across different age groups. B) Comparison of the numbers and percentages of TM in mice at different ages. Data are presented as mean ± SEM (n = 4-12 per group from 2-4 independent experiments).

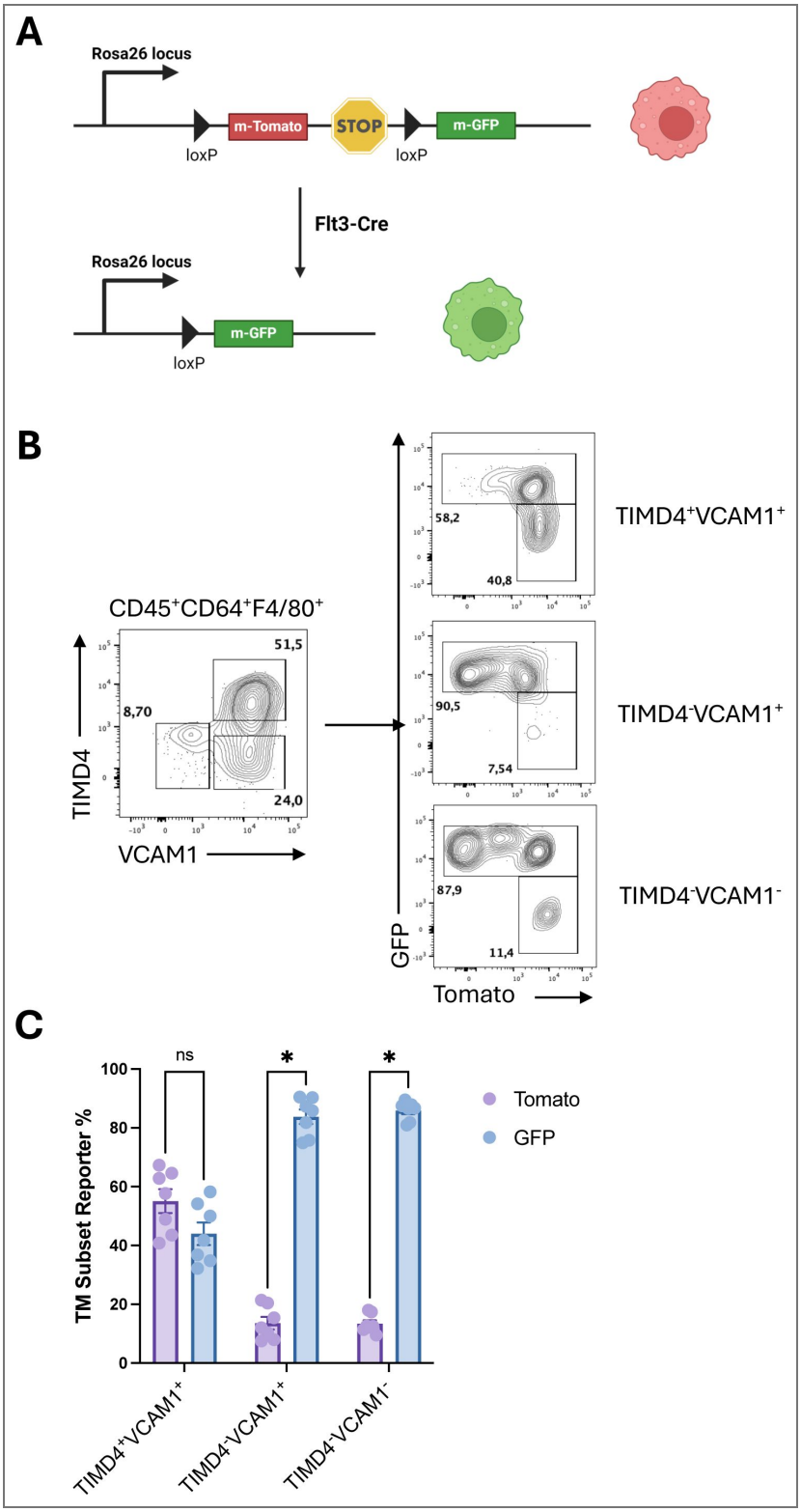


**Figure 6. Ontology of TM subsets.**

Thymuses were harvested from 11–14-week-old *Flt3*-Cre × *Rosa*-mTmG mice and enzymatically digested to obtain single-cell suspensions. Cells were stained with antibodies for flow cytometric analysis. A) Schematic representation of the *Flt3*-Cre × *Rosa*-mTmG reporter mouse model. B) Representative flow cytometry plots showing mTomato (Tomato) and mGFP (GFP) reporter expression across TIMD4$^+$VCAM1$^+$, TIMD4$^-$VCAM1$^+$, and TIMD4$^-$ VCAM1$^-$ subsets. C) Comparison of reporter expression percentages among TM subsets. Data are presented as mean ± SEM (n = 7 per group from 2 independent experiments). Statistical significance was assessed using the Mann-Whitney test for pairwise comparisons, followed by the Holm-Šídá method to correct for multiple comparisons (***p ≤ 0.001).

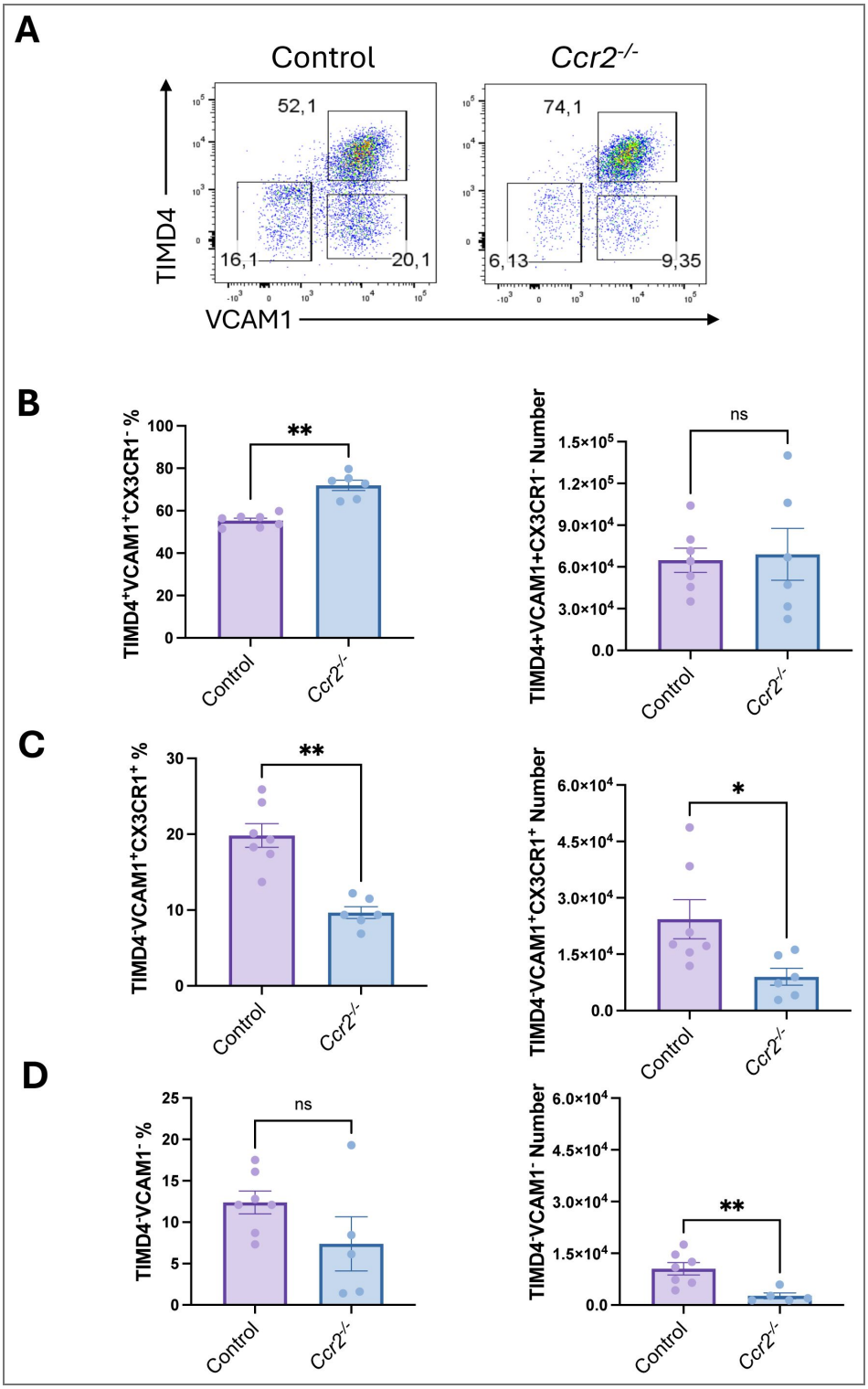


**Figure 7. TIMD4$^-$VCAM1$^+$ TM subset is HSC derived.**

Thymuses were harvested from 11–14-week-old *Flt3*-Cre × *Rosa*-mTmG mice (Control) and *Flt3*-Cre × *Rosa*-mTmG mice in the CCR2 knockout background (*Ccr2*$^{-/-}$), followed by enzymatic digestion to prepare single-cell suspensions. Cells were stained with antibodies for flow cytometric analysis. A) Representative flow cytometry plots showing TM subsets from *Ccr2*$^{-/-}$ and control mice. B) Comparison of TIMD4$^+$VCAM1$^+$ TM subset percentage and absolute numbers between *Ccr2*$^{-/-}$ and control mice. C) Comparison of TIMD4$^-$VCAM1$^+$ TM subset percentage and absolute numbers between *Ccr2*$^{-/-}$ and control mice. D) Comparison of TIMD4$^-$VCAM1$^-$ TM percentage and absolute numbers between *Ccr2*$^{-/-}$ and control mice. Data are presented as mean ± SEM (n = 6–7 per group from 2 independent experiments). Statistical significance was assessed using a two-tailed Mann-Whitney test (*p ≤ 0.05, **p ≤ 0.01, and ***p ≤ 0.001).

Together, these data establish a dual-origin model for the thymic macrophage network: a stable, self-maintaining population of TIMD4$^+$ VCAM1$^+$ CX3CR1$^-$ macrophages established from fetal, FLT3-independent precursors, which coexists with a dynamic, CCR2-dependent population of TIMD4$^-$ VCAM1$^+$ CX3CR1$^+$ macrophages that is continuously replenished by circulating monocytes.

### Depletion of Csf1r-Expressing Myeloid Cells in Thymic Organ Culture Impairs T Cell Development at the β-Selection Checkpoint

To directly test the functional requirement for TMs during T cell development, we employed the MaFIA (Csf1r-EGFP/Fas-FKBP) mouse model, which permits the inducible depletion of Csf1r-expressing cells (Supplemental Figure 2A-B) (37). Because both TM subsets and thymic monocytes express the Csf1r-EGFP reporter, this system enables the targeted depletion of the thymic myeloid compartment (Supplemental Figure 2C-E). To circumvent the systemic effects of *in vivo* depletion, we utilized an *ex vivo* fetal thymic organ culture (FTOC) system (38). Thymic lobes from E15.5 MaFIA embryos were cultured with the dimerizer drug AP20187 to induce apoptosis in *Csf1r*$^+$ cells (Figure 8A).

To validate the specificity of our approach, we first examined the non-myeloid stromal compartment. Flow cytometry analysis confirmed that the number of TECs, identified as EpCAM$^+$ CD45$^-$, appeared unaffected by the treatment (Figure 8B). In contrast, depletion was highly effective against the intended myeloid targets. We observed a significant reduction in the total number of thymocytes and thymic DCs (Figure 8C-D). Crucially, the treatment also resulted in the profound loss of total TMs (Figure 8E). This effect was specific to the MaFIA system, as treatment of control C57BL/6 mice with the dimerizer did not cause TM depletion (Figure 8F). Analysis of the TM populations revealed that both the TIMD4$^+$ VCAM1$^+$ CX3CR1$^-$ and the TIMD4$^-$ VCAM1$^+$ CX3CR1$^+$ subsets were significantly depleted (Figure 8G-H).

Depletion of *Csf1r*$^+$ cells led to an impairment in αβ T cell development (Figure 9A). AP20187-treated thymic lobes exhibited a significant reduction in the number of CD4$^+$ CD8$^+$ DP thymocytes (Figure 9B-C). While the development of γδ T cells was unaffected (Figure 9D). To identify the origin of this defect, we analyzed the upstream DN progenitor stages (Figure 10A). This revealed a developmental block, as treated FTOCs showed a significant accumulation of DN3 (CD44$^-$ CD25$^+$) thymocytes and a corresponding decrease in the subsequent DN4 (CD44$^-$ CD25$^-$) population (Figure 10B).

To pinpoint the impairment more precisely, we examined the expression of CD27, a surface marker upregulated upon successful pre-TCR signaling. Within the arrested DN3 population of treated lobes, the proportion of CD27$^+$ cells was significantly reduced (Figure 10C-D). This points to a failure of thymocytes to receive or transduce the signals required to pass the β-selection checkpoint. Collectively, these data reveal that the *Csf1r*-expressing myeloid compartment, which includes thymic macrophages, appears to be important for the successful transition of thymocytes through β-selection, a critical early checkpoint in T cell development.

## Discussion

The thymus provides a unique and specialized niche for T cell development, yet the contributions of its resident myeloid populations have been historically underappreciated. This study redefines the role of TMs, moving beyond their established function as mere "housekeepers" to reveal them as a heterogeneous and dynamic population that also is integral for the earliest checkpoints in T cell development. By combining high-resolution phenotyping, fate-mapping, and functional depletion, we demonstrate that the thymus contains two distinct macrophage subsets with separate origins and functions, and we uncover a critical role for the myeloid compartment in supporting thymocyte progression through β-selection.

Our work addresses the complexity of the TM landscape by integrating flow cytometry and single-cell transcriptomics. We identified a dominant TIMD4$^+$ VCAM1$^+$ CX3CR1$^-$ population transcriptionally programmed for efferocytosis, expressing high levels of *Mertk* and sharing a gene signature (*Spic*, *MafB*) with splenic red pulp macrophages (36). However, using *Spic* knockout

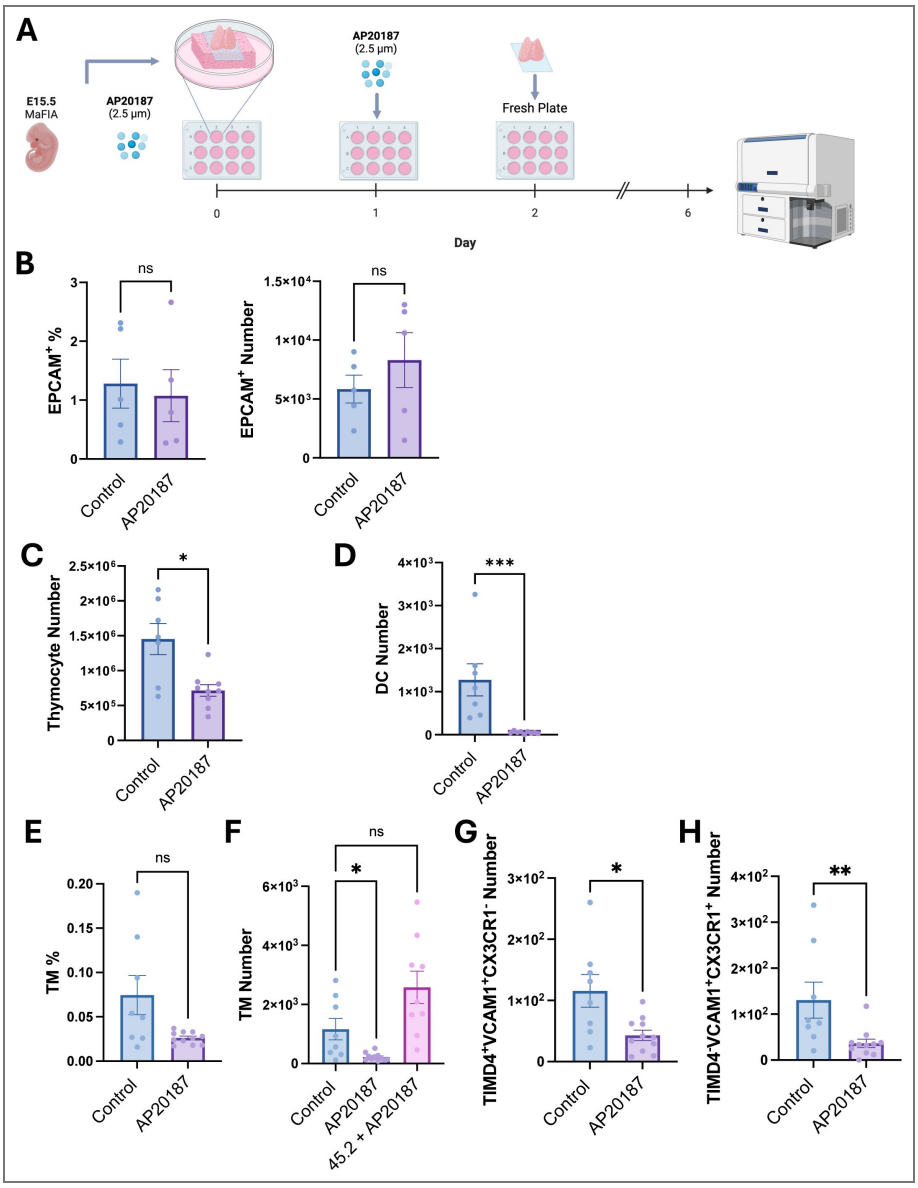


**Figure 8. FTOC analysis of TM function during T cell development in MaFIA mice.**

Thymuses from E15.5 MaFIA mice were used to establish FTOCs. Cultures were treated with 2.5 mM AP20187 to deplete *Csf1r*-expressing cells on the day of setup and again the following day. On day 2, FTOC films were transferred to fresh media plates, and samples were analyzed by flow cytometry on day 6 to assess T cell development kinetics. A) Schematic representation of the TMs depletion workflow in FTOC culture. B) Percentages and absolute numbers of EPCAM$^+$ cells in FTOC samples on day 2, comparing control and AP20187-treated groups, analyzed by flow cytometry. C) Total thymocyte numbers on day 6, comparing control and AP20187-treated groups. D) Absolute numbers of DCs on day 6, comparing control and AP20187-treated groups. DCs were gated as CD45$^+$CD11c$^+$MHC-II$^{hi}$. Data are presented as mean ± SEM (n = 8–11 per group from 3 independent experiments). Statistical significance was assessed using a two-tailed Mann-Whitney test (*p ≤ 0.05 and ***p ≤ 0.001). E) Thymuses from embryonic day 15.5 (E15.5) MaFIA (*Csf1r*-EGFP) and congenic C57BL/6 (45.2) mice were used to setup FTOCs. Cultures were treated with 2.5 mM AP20187 to deplete *Csf1r*-expressing cells on the day of setup and again the following day. On day 2, FTOC films were transferred to fresh media plates, and samples were analyzed by flow cytometry on day 6 to assess T cell development kinetics. Comparison of TM percentages between control and AP20187-treated MaFIA mice. F) Comparison of TM absolute numbers in control and AP20187-treated MaFIA FTOCs, as well as in AP20187-treated C57BL/6 FTOCs. G) Comparison of TIMD4$^+$VCAM1$^+$CX3CR1$^-$ numbers between control and AP20187-treated MaFIA mice. H) Comparison of TIMD4$^-$VCAM1$^+$CX3CR1$^+$ numbers between control and AP20187-treated MaFIA mice. Data are presented as the mean ± SEM (n = 8–11 per group from 3 independent experiments). Statistical significance was assessed using a two-tailed Mann-Whitney test (*p ≤ 0.05 and **p ≤ 0.01) for comparisons between two groups. A Kruskal-Wallis test was performed for multiple comparisons between three groups (*p ≤ 0.05).

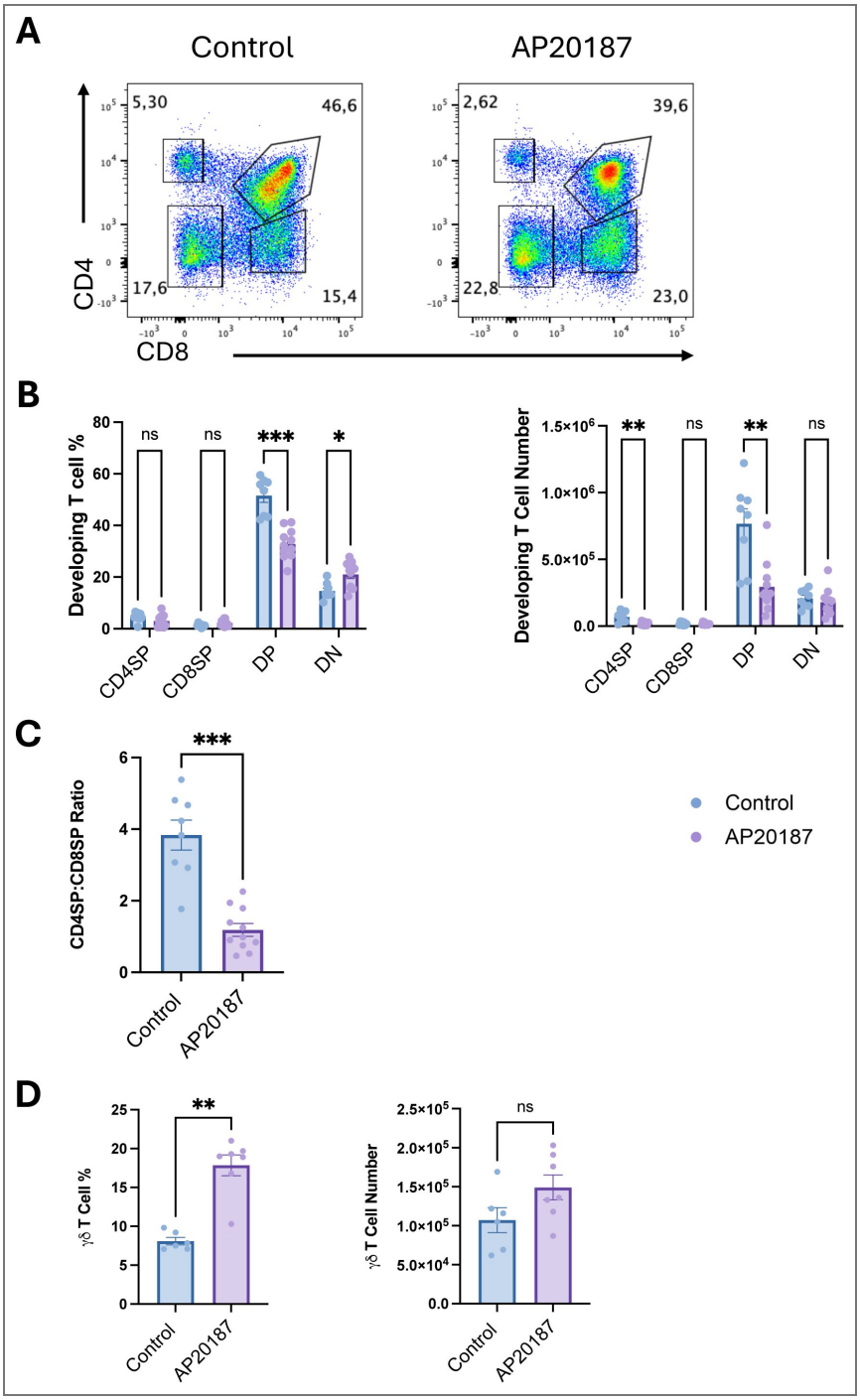


**Figure 9. Impairment of T cell development in the absence of TMs.**

Thymuses from embryonic day 15.5 (E15.5) MaFIA mice were used to establish FTOCs. Cultures were treated with 2.5 mM AP20187 to deplete *Csf1r*-expressing cells on the day of setup and again the following day. On day 2, FTOC films were transferred to fresh media plates, and samples were analyzed by flow cytometry on day 6 to assess T cell development kinetics. A) Representative flow cytometry plot showing T cell populations defined by CD4 and CD8 markers. B) Comparison of percentages and absolute numbers of developing T cells between control and AP20187-treated FTOC samples. C) Ratio of $CD3^+CD4^+$ single-positive (CD4SP) to $CD3^+CD8^+$ single-positive (CD8SP) thymocytes in control versus AP20187-treated FTOCs. Data are presented as the mean ± SEM (n = 8–11 per group from 3 independent experiments). D) Comparison of percentage and absolute numbers of γδ T cells between control and AP20187-treated FTOC samples. Data are presented as the mean ± SEM (n = 6–7 per group from 2 independent experiments). Statistical significance was assessed using the Mann-Whitney test, followed by the Holm-Šídák method to correct for multiple comparisons (*p ≤ 0.05, **p ≤ 0.01, and ***p ≤ 0.001).

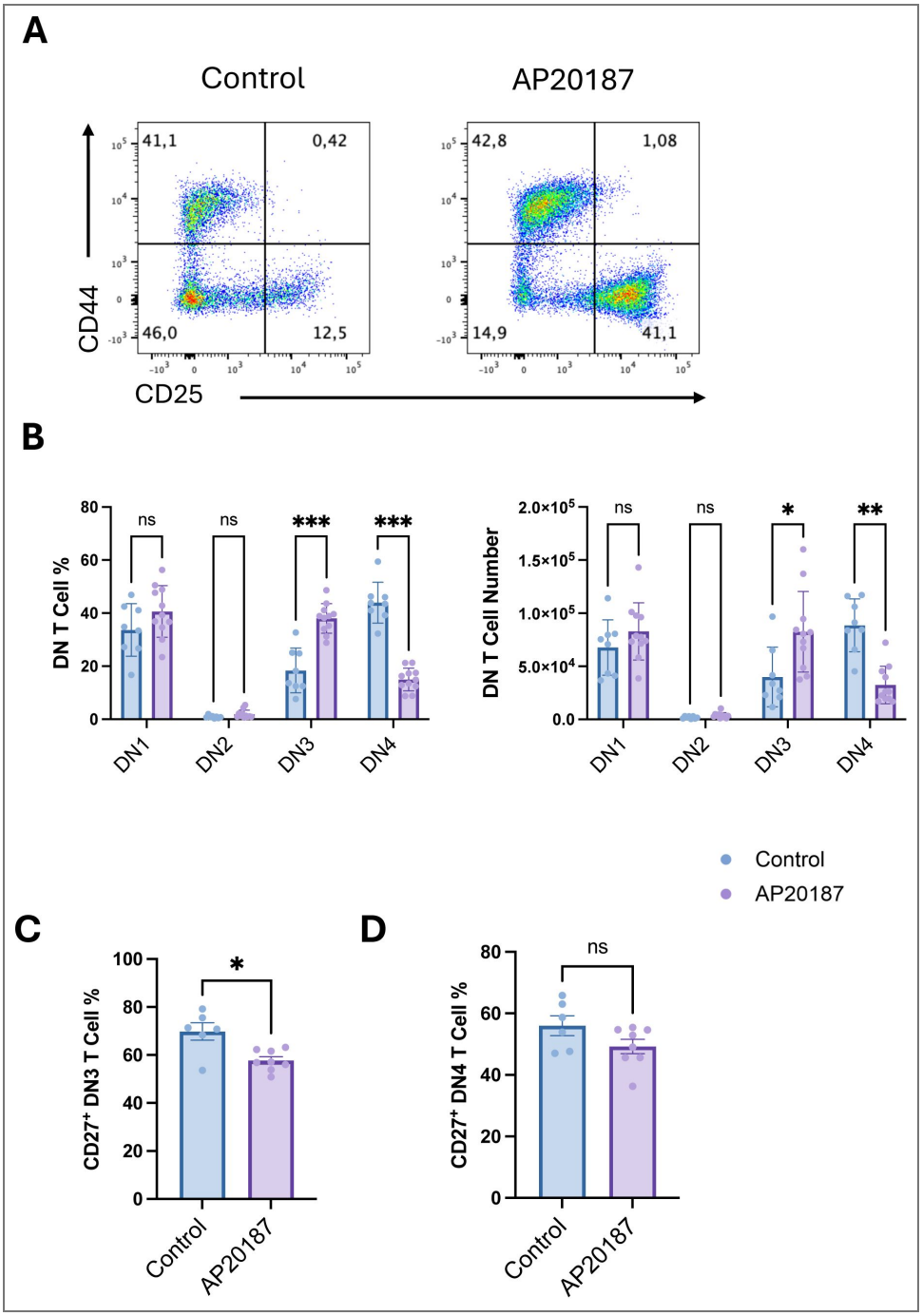


**Figure 10. TMs are critical for β-selection during T cell development.**

Thymuses from embryonic day 15.5 (E15.5) MaFIA mice were used to establish FTOCs. Cultures were treated with 2.5 mM AP20187 to deplete *Csf1r*-expressing cells on the day of setup and again the following day. On day 2, FTOC films were transferred to fresh media plates, and samples were analyzed by flow cytometry on day 6 to assess T cell development kinetics. A) Representative flow cytometry plot showing DN cell populations defined by CD44 and CD25 markers B) Comparison of percentages and absolute numbers of DN cells between control and AP20187-treated FTOC samples. Data are presented as mean ± SEM (n = 8–11 per group from 3 independent experiments). C) Comparison of $CD27^+$ DN3 cells percentage between control and AP20187-treated FTOC samples. D) Comparison of $CD27^+$ DN4 cells percentage between control and AP20187-treated FTOC samples. Data are presented as mean ± SEM (n = 6–8 per group from 2 independent experiments). Statistical significance was assessed using the Mann-Whitney test for pairwise comparisons, followed by the Holm-Šídá method to correct for multiple comparisons (*p ≤ 0.05, **p ≤ 0.01, and ***p ≤ 0.001).

mice, we showed that TMs, unlike their splenic counterparts, follow a *Spic*-independent developmental pathway, highlighting their unique adaptation to the thymic niche. In contrast, the TIMD4$^-$ VCAM1$^+$ CX3CR1$^+$ subset was enriched for genes involved in antigen presentation and interferon signaling, positioning it as a candidate for shaping the T cell repertoire, a role previously attributed almost exclusively to DCs (20).

Furthermore, we establish a dual-origin model for this network. The homeostatic TIMD4$^+$ VCAM1$^+$ CX3CR1$^-$ macrophages are likely long-lived, self-maintaining cells derived from embryonic, FLT3-independent precursors. Conversely, the TIMD4$^-$ VCAM1$^+$ CX3CR1$^+$ subset is continuously replenished from HSC-derived, Flt3-dependent monocytes, representing a more dynamic population likely involved in immune surveillance (39,40). This clarifies conflicting reports in the literature and aligns TM biology with the broader principles of tissue-resident macrophage ontogeny observed in other organs (23,27).

An impactful finding of this study is the appreciation of novel role for thymic myeloid cells in early T cell development. Using an *ex vivo* FTOC system to avoid the confounding stress of *in vivo* depletion, we demonstrated that the loss of *Csf1r*-expressing cells leads to a profound developmental block at the DN3 to DN4 transition. The accumulation of DN3 cells, coupled with a specific reduction in CD27 expression, pinpoints a failure at the β-selection checkpoint (41,42). While traditionally viewed as a cell-autonomous event, our data strongly suggest that pre-TCR signaling is not independent of the microenvironment (12). This support from myeloid cells could be multifaceted, involving the presentation of peptide-MHC to the pre-TCR (43–45) or other receptor-ligand interactions, the provision of essential survival factors (46–48), or the maintenance of a non-inflammatory niche through the clearance of apoptotic cells (49).

Although our depletion strategy also affected DCs, several lines of evidence implicate TMs as the primary mediators of this effect. The β-selection checkpoint occurs in the thymic cortex, a region densely populated by TMs, whereas DCs are largely restricted to the medulla and cortico-medullary junction (50). Nevertheless, future studies using more targeted depletion strategies will be crucial to definitively dissect the relative contributions of TMs and DCs. Additionally, the absence of TMs might lead to an accumulation of apoptotic cells, creating a potentially hostile environment for early thymocyte development. Macrophages, through their role in clearing apoptotic cells, produce anti-inflammatory cytokines like IL-10 and TGF-β, while suppressing pro-inflammatory cytokines such as IL-12 (51–53). Without these regulatory influences, TM depletion may result in localized thymic inflammation, further compromising thymocyte survival and development (54). Together, these findings highlight a supportive role of TMs in β-selection, not only by facilitating essential pre-TCR interactions but also by preserving a supportive microenvironment for thymocyte maturation.

In conclusion, this study elevates thymic macrophages from simple scavengers to critical architects of the initial TCRβ repertoire. By defining their heterogeneity, origins, and functional specialization, we reveal their integral role in thymic homeostasis and uncover their essential contribution to the successful navigation of the earliest checkpoints in T cell development. These findings not only advance our fundamental understanding of thymic biology but also open new avenues for exploring how modulation of this myeloid niche could influence immune tolerance and T cell-based therapies.

## Data availability

Single cell RNAseq datasets have been deposited to the Gene Expression Omnibus (GEO) repository, accession number GSE326594.

# Supplemental Figures

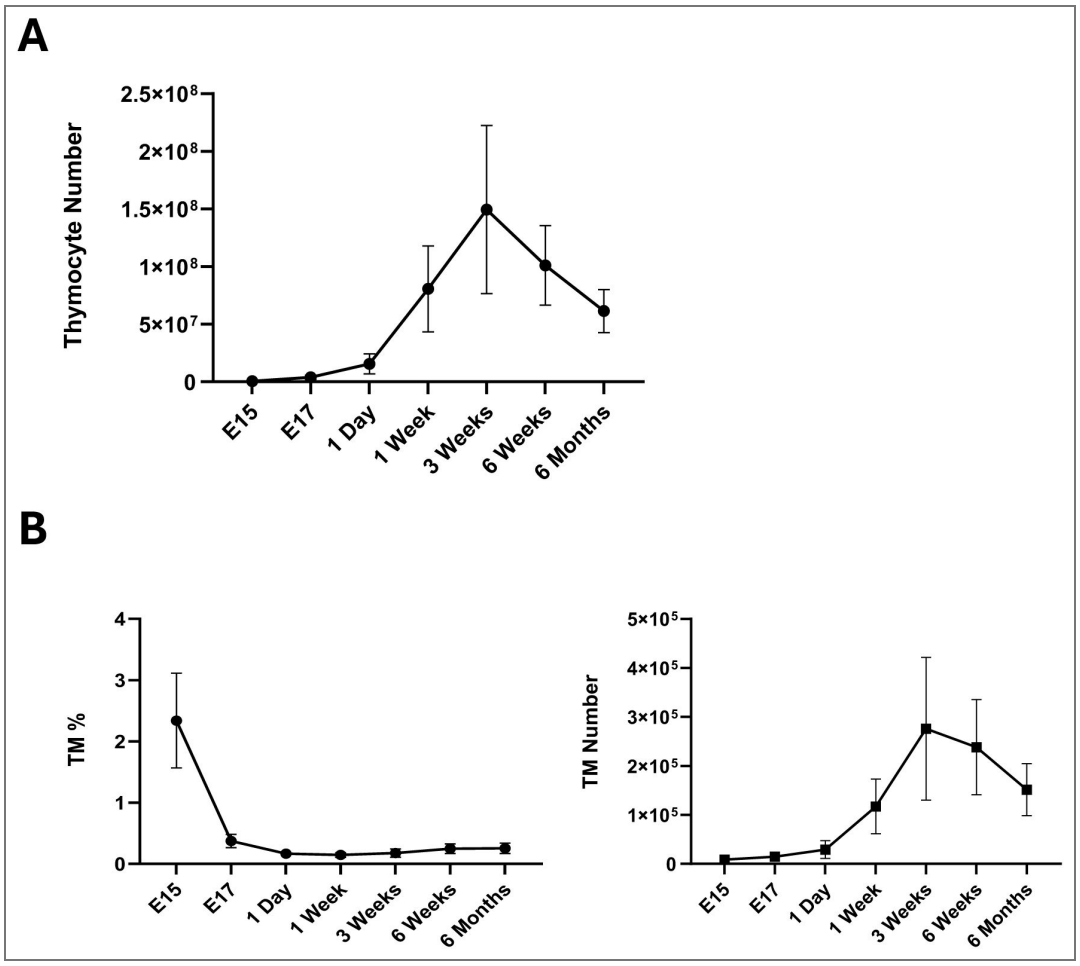


**Supplemental Figure 1. Changes in TM numbers during thymic development.** Thymuses were harvested from mouse at various developmental time points and enzymatically digested to obtain single-cell suspensions. Cells were stained with antibodies for flow cytometry analysis. A) Total thymocyte numbers at different ages. B) Comparison of TM numbers and percentages across different ages of mice. Data are presented as mean ± SEM (n = 6-12 per group from 2-4 independent experiments).

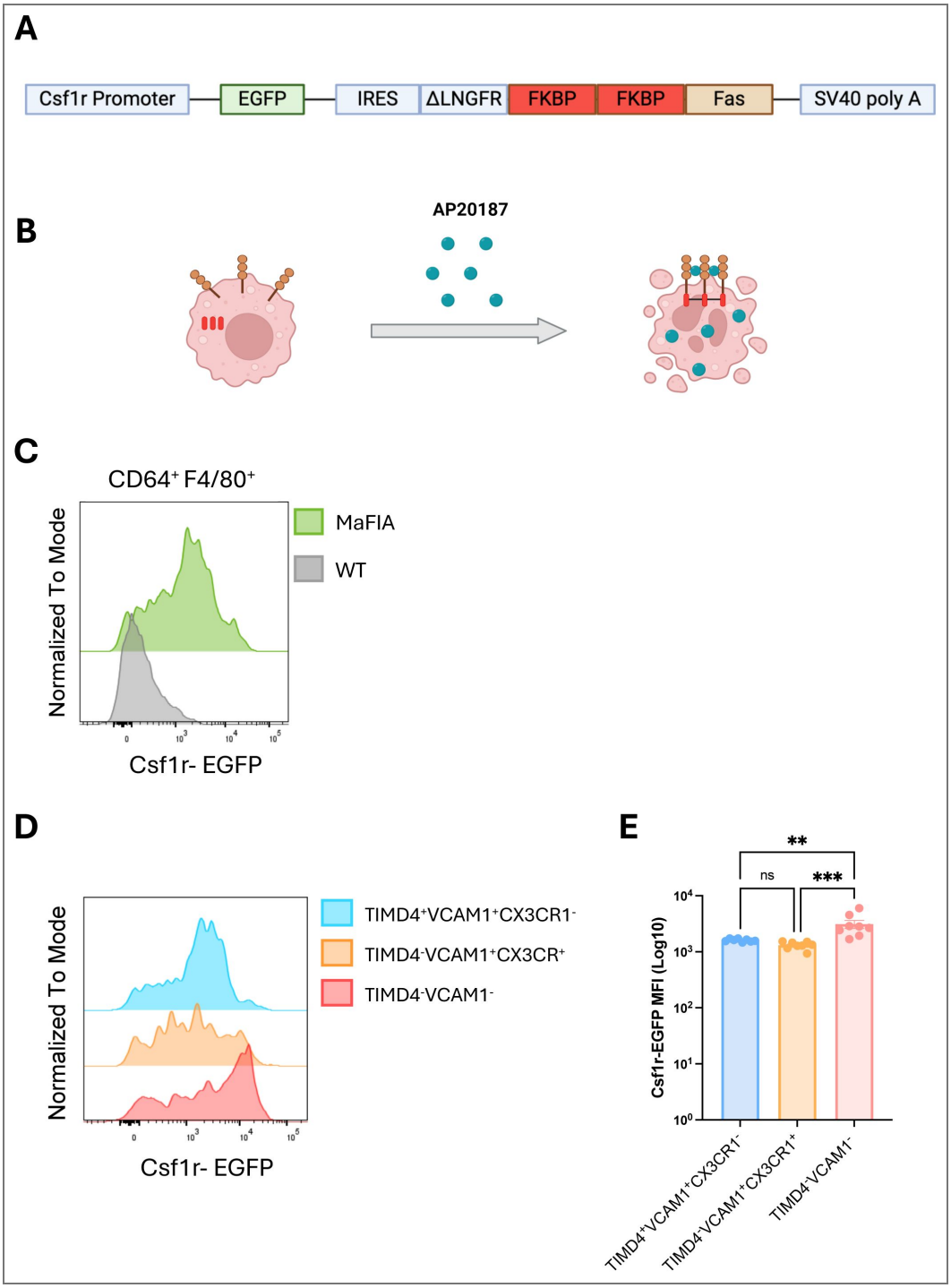


**Supplemental Figure 2. TM analysis in MaFIA mice.**

Thymuses were harvested from six-week-old MaFIA mice and enzymatically digested for single-cell preparation. Cells were stained with antibodies for flow cytometric analysis. A) Schematic representation of the transgene elements in the MaFIA mouse strain. B) Schematic representation of the mechanism by which AP20187 binds FKBP-expressing cells, leading to the induction of apoptosis. C) Representative images showing *Csf1r*-GFP reporter expression in TMs from MaFIA TM (green) and C75BL/6J (WT) TMs (grey) mice. D) Representative histogram showing *Csf1r*-EGFP reporter expression across $TIMD4^{+}VCAM1^{+}CX3CR1^{-}$, $TIMD4^{-}VCAM1^{+}CX3CR1^{+}$, and $TIMD4^{-}VCAM1^{-}$ TM subsets. E) Comparison of *Csf1r*-EGFP means fluorescence intensity (MFI) across $TIMD4^{+}VCAM1^{+}CX3CR1^{-}$, $TIMD4^{-}VCAM1^{+}CX3CR1^{+}$, and $TIMD4^{-}VCAM1^{-}$ TM subsets. Data are presented as mean ± SEM (n = 4 per group from 2 independent experiments). A Kruskal-Wallis test was performed for multiple comparisons between three groups (**p ≤ 0.01).

# Additional information

## Funding


| Funder | Grant reference number | Author |
|---|---|---|
| Canadian Institutes of Health Research (CIHR) | FDN154332 | Juan Carlos Zúñiga-Pflücker |
| Canadian Institutes of Health Research (CIHR) | PJT192050 | Juan Carlos Zúñiga-Pflücker |
| Natural Sciences and Engineering Research Council of Canada (NSERC) | RGPIN-2024-05661 | Juan Carlos Zúñiga-Pflücker |
| Canadian Institutes of Health Research (CIHR) | Postdoctoral Fellowship | Vinothkumar Rajan |


## Author ORCID iDs

**Juan Carlos Zúñiga-Pflücker**: https://orcid.org/0000-0003-2538-3178

# References


1. **Miller JFAP** (2011) The golden anniversary of the thymus. *Nat Rev Immunol* **11**:489-95 https://doi.org/10.1038/nri2993 | PubMed
2. **Shah DK,** Zuniga-Pflucker JC (2014) An Overview of the Intrathymic Intricacies of T Cell Development. *J Immunol* **192**:4017-23 https://doi.org/10.4049/jimmunol.1302259 | PubMed
3. **James KD,** Jenkinson WE, Anderson G (2021) Non-Epithelial Stromal Cells in Thymus Development and Function. *Front Immunol* **12**:634367 https://doi.org/10.3389/fimmu.2021.634367 | PubMed
4. **Petrie HT,** Zúñiga-Pflücker JC (2007) Zoned out: functional mapping of stromal signaling microenvironments in the thymus. *Annu Rev Immunol* **25**:649-79 https://doi.org/10.1146/annurev.immunol.23.021704.115715 | PubMed
5. **Foss DL,** Donskoy E, Goldschneider I (2001) The Importation of Hematogenous Precursors by the Thymus Is a Gated Phenomenon in Normal Adult Mice. *J Exp Med* **193**:365-74 https://doi.org/10.1084/jem.193.3.365 | PubMed
6. **Studies of thymocytopoiesis in rats and mice. I.** (1986) Kinetics of appearance of thymocytes using a direct intrathymic adoptive transfer assay for thymocyte precursors. *J Exp Med* **163**:1-17 https://doi.org/10.1084/jem.163.1.1 | PubMed
7. **Benz C,** Martins VC, Radtke F, Bleul CC (2008) The stream of precursors that colonizes the thymus proceeds selectively through the early T lineage precursor stage of T cell development. *J Exp Med* **205**:1187-99 https://doi.org/10.1084/jem.20072168 | PubMed
8. **Ciofani M,** Zúñiga-Pflücker JC (2010) Determining γδ versus αβ T cell development. *Nat Rev Immunol* **10**:657-63 https://doi.org/10.1038/nri2820 | PubMed
9. **Moran AE,** Hogquist KA (2012) T-cell receptor affinity in thymic development. *Immunology* **135**:261-7 https://doi.org/10.1111/j.1365-2567.2011.03547.x | PubMed
10. **Willerford DM,** Swat W, Alt FW (1996) Developmental regulation of V(D)J recombination and lymphocyte differentiation. *Curr Opin Genet Dev* **6**:603-9 https://doi.org/10.1016/s0959-437x(96)80090-6 | PubMed
11. **Shinkai Y,** Rathbun G, Lam KP, Oltz EM, Stewart V, Mendelsohn M, et al. (1992) RAG-2-deficient mice lack mature lymphocytes owing to inability to initiate V(D)J rearrangement. *Cell* **68**:855-67 https://doi.org/10.1016/0092-8674(92)90029-c | PubMed
12. **Michie AM,** Zúñiga-Pflücker JC (2002) Regulation of thymocyte differentiation: pre-TCR signals and *β*-selection. *Semin Immunol* **14**:311-23 https://doi.org/10.1016/s1044-5323(02)00064-7 | PubMed

13. **Das DK,** Mallis RJ, Duke-Cohan JS, Hussey RE, Tetteh PW, Hilton M, et al. (2016) Pre-T Cell Receptors (Pre-TCRs) Leverage Vβ Complementarity Determining Regions (CDRs) and Hydrophobic Patch in Mechanosensing Thymic Self-ligands. *J Biol Chem* **291**:25292-305 https://doi.org/10.1074/jbc.m116.752865 | PubMed

14. **Falk I,** Nerz G, Haidl I, Krotkova A, Eichmann K (2001) Immature thymocytes that fail to express TCRbeta and/or TCRgamma delta proteins die by apoptotic cell death in the CD44(-)CD25(-) (DN4) subset. *Eur J Immunol* **31**:3308-17 https://doi.org/10.1002/1521-4141(200111)31:11<3308::aid-immu3308>3.0.co;2-5 | PubMed

15. **Rothenberg EV,** Moore JE, Yui MA (2008) Launching the T-Lineage Developmental Programme. *Nat Rev Immunol* **8**:9-21 https://doi.org/10.1038/nri2232 | PubMed

16. **Klein L,** Petrozziello E (2025) Antigen presentation for central tolerance induction. *Nat Rev Immunol* **25**:57-72 https://doi.org/10.1038/s41577-024-01076-8 | PubMed

17. **Charles A,** Janeway J, Travers P, Walport M, Shlomchik MJ (2001) T-cell receptor gene rearrangement. Immunobiol Immune Syst Health Dis 5th Ed. https://www.ncbi.nlm.nih.gov/books/NBK27145/

18. **Murata S,** Takahama Y, Tanaka K (2008) Thymoproteasome: probable role in generating positively selecting peptides. *Curr Opin Immunol* **20**:192-6 https://doi.org/10.1016/j.coi.2008.03.002 | PubMed

19. **Gotter J,** Brors B, Hergenhahn M, Kyewski B (2004) Medullary epithelial cells of the human thymus express a highly diverse selection of tissue-specific genes colocalized in chromosomal clusters. *J Exp Med* **199**:155-66 https://doi.org/10.1084/jem.20031677 | PubMed

20. **Proietto AI,** van Dommelen S, Zhou P, Rizzitelli A, D'Amico A, Steptoe RJ, et al. (2008) Dendritic cells in the thymus contribute to T-regulatory cell induction. *Proc Natl Acad Sci U S A* **105**:19869-74 https://doi.org/10.1073/pnas.0810268105 | PubMed

21. **Palmer E** (2003) Negative selection — clearing out the bad apples from the T-cell repertoire. *Nat Rev Immunol* **3**:383-91 https://doi.org/10.1038/nri1085 | PubMed

22. **Klein L,** Kyewski B, Allen PM, Hogquist KA (2014) Positive and negative selection of the T cell repertoire: what thymocytes see (and don't see). *Nat Rev Immunol* **14**:377-91 https://doi.org/10.1038/nri3667 | PubMed

23. **Hanna RN,** Carlin LM, Hubbeling HG, Nackiewicz D, Green AM, Punt JA, et al. (2011) The transcription factor NR4A1 (Nur77) controls bone marrow differentiation and survival of Ly6C– monocytes. *Nat Immunol* **12**:778 https://doi.org/10.1038/ni.2063 | PubMed

24. **Baratin M,** Simon L, Jorquera A, Ghigo C, Dembele D, Nowak J, et al. (2017) T Cell Zone Resident Macrophages Silently Dispose of Apoptotic Cells in the Lymph Node. *Immunity* **47**:349-362. https://doi.org/10.1016/j.immuni.2017.07.019 | PubMed

25. **Wang H,** Zúñiga-Pflücker JC (2022) Thymic Microenvironment: Interactions Between Innate Immune Cells and Developing Thymocytes. *Front Immunol* **13**:885280 https://doi.org/10.3389/fimmu.2022.885280 | PubMed

26. **Italiani P,** Boraschi D (2014) From Monocytes to M1/M2 Macrophages: Phenotypical vs. Functional Differentiation. *Front Immunol* **5**:514 https://doi.org/10.3389/fimmu.2014.00514 | PubMed

27. **Zhou TA,** Hsu HP, Tu YH, Lin CY, Chen NJ, Tsai JW, et al. (2021) Thymic macrophages consist of two populations with distinct localization and origi. *bioRxiv* https://doi.org/10.1101/2021.11.04.467238

28. **Epelman S,** Lavine KJ, Beaudin AE, Sojka DK, Carrero JA, Calderon B, et al. (2014) Embryonic and adult-derived resident cardiac macrophages are maintained through distinct mechanisms at steady state and during inflammation. *Immunity* **40**:91-104 https://doi.org/10.1016/j.immuni.2013.11.019 | PubMed

29. **Han J,** Zúñiga-Pflücker JC (2021) High-Oxygen Submersion Fetal Thymus Organ Cultures Enable FOXN1-Dependent and -Independent Support of T Lymphopoiesis. *Front Immunol* **12** https://doi.org/10.3389/fimmu.2021.652665 | PubMed

30. **Nitta T,** Ohigashi I, Takahama Y (2013) The Development of T Lymphocytes in Fetal Thymus Organ Culture. In: Helgason CD, Miller CL (Eds). *Basic Cell Culture Protocols* Totowa, NJ: Humana Press. pp. 85-102 https://doi.org/10.1007/978-1-62703-128-8_6

31. **Satija R,** Farrell JA, Gennert D, Schier AF, Regev A (2015) Spatial reconstruction of single-cell gene expression data. *Nat Biotechnol* **33**:495-502 https://doi.org/10.1038/nbt.3192 | PubMed

32. **Dick SA,** Wong A, Hamidzada H, Nejat S, Nechanitzky R, Vohra S, et al. (2022) Three tissue resident macrophage subsets coexist across organs with conserved origins and life cycles. *Sci Immunol* **7**:eabf7777 https://doi.org/10.1126/sciimmunol.abf7777 | PubMed

33. **Korsunsky I,** Millard N, Fan J, Slowikowski K, Zhang F, Wei K, et al. (2019) Fast, sensitive and accurate integration of single-cell data with Harmony. *Nat Methods* **16**:1289-96 https://doi.org/10.1038/s41592-019-0619-0 | PubMed

34. **Trapnell C,** Cacchiarelli D, Grimsby J, Pokharel P, Li S, Morse M, et al. (2014) The dynamics and regulators of cell fate decisions are revealed by pseudotemporal ordering of single cells. *Nat Biotechnol* **32**:381-6 https://doi.org/10.1038/nbt.2859 | PubMed

35. **Thorp E,** Cui D, Schrijvers DM, Kuriakose G, Tabas I (2008) Mertk Receptor Mutation Reduces Efferocytosis Efficiency and Promotes Apoptotic Cell Accumulation and Plaque Necrosis in Atherosclerotic Lesions of Apoe−/− Mice. *Arterioscler Thromb Vasc Biol* **28**:1421-8 https://doi.org/10.1161/atvbaha.108.167197 | PubMed

36. **Kohyama M,** Ise W, Edelson BT, Wilker PR, Hildner K, Mejia C, et al. (2009) Critical role for Spi-C in the development of red pulp macrophages and splenic iron homeostasis. *Nature* **457**:318-21 https://doi.org/10.1038/nature07472 | PubMed

37. **Burnett SH,** Kershen EJ, Zhang J, Zeng L, Straley SC, Kaplan AM, et al. (2004) Conditional macrophage ablation in transgenic mice expressing a Fas-based suicide gene. *J Leukoc Biol* **75**:612-23 https://doi.org/10.1189/jlb.0903442 | PubMed

38. **Jenkinson EJ,** Anderson G (1994) Fetal thymic organ cultures. *Curr Opin Immunol* **6**:293-7 https://doi.org/10.1016/0952-7915(94)90104-x | PubMed

39. **Bain CC,** Bravo-Blas A, Scott CL, Gomez Perdiguero E, Geissmann F, Henri S, et al. (2014) Constant replenishment from circulating monocytes maintains the macrophage pool in the intestine of adult mice. *Nat Immunol* **15**:929-37 https://doi.org/10.1038/ni.2967 | PubMed

40. **Davies LC,** Rosas M, Smith PJ, Fraser DJ, Jones SA, Taylor PR (2011) A quantifiable proliferative burst of tissue macrophages restores homeostatic macrophage populations after acute inflammation. *Eur J Immunol* **41**:2155-64 https://doi.org/10.1002/eji.201141817 | PubMed

41. **Boehmer H von,** Fehling HJ (1997) Structure and function of the pre-t cell receptor. *Annu Rev Immunol* **15**:433-52 https://doi.org/10.1146/annurev.immunol.15.1.433 | PubMed

42. **Taghon T,** Yui MA, Pant R, Diamond RA, Rothenberg EV (2006) Developmental and Molecular Characterization of Emerging β- and γδ-Selected Pre-T Cells in the Adult Mouse Thymus. *Immunity* **24**:53-64 https://doi.org/10.1016/j.immuni.2005.11.012 | PubMed

43. **Duke-Cohan JS,** Akitsu A, Mallis RJ, Messier CM, Lizotte PH, Aster JC, et al. (2023) Pre-T cell receptor self-MHC sampling restricts thymocyte dedifferentiation. *Nature* **613**:565-74 https://doi.org/10.1038/s41586-022-05555-7 | PubMed

44. **Li X,** Mizsei R, Tan K, Mallis RJ, Duke-Cohan JS, Akitsu A, et al. (2021) Pre-T cell receptors topologically sample self-ligands during thymocyte β-selection. *Science* **371**:181-5 https://doi.org/10.1126/science.abe0918 | PubMed

45. **Mizsei R,** Li X, Chen WN, Szabo M, Wang JH, Wagner G, et al. (2021) A general chemical crosslinking strategy for structural analyses of weakly interacting proteins applied to preTCR-pMHC complexes. *J Biol Chem* **296**:100255 https://doi.org/10.1016/j.jbc.2021.100255 | PubMed

46. **Ciofani M,** Knowles GC, Wiest DL, von Boehmer H, Zúñiga-Pflücker JC (2006) Stage-specific and differential notch dependency at the alphabeta and gammadelta T lineage bifurcation. *Immunity* **25**:105-16 https://doi.org/10.1016/j.immuni.2006.05.010 | PubMed

47. **Ciofani M,** Schmitt TM, Ciofani A, Michie AM, Çuburu N, Aublin A, et al. (2004) Obligatory Role for Cooperative Signaling by Pre-TCR and Notch during Thymocyte Differentiation1. *J Immunol* **172**:5230-9 https://doi.org/10.4049/jimmunol.172.9.5230 | PubMed

48. **Ciofani M,** Zúñiga-Pflücker JC (2005) Notch promotes survival of pre-T cells at the beta-selection checkpoint by regulating cellular metabolism. *Nat Immunol* **6**:881-8 https://doi.org/10.1038/ni1234 | PubMed

49. **Bernhard CA,** Ried C, Kochanek S, Brocker T (2015) CD169+ macrophages are sufficient for priming of CTLs with specificities left out by cross-priming dendritic cells. *Proc Natl Acad Sci* **112**:5461-6 https://doi.org/10.1073/pnas.1423356112 | PubMed

50. **Hadeiba H,** Lahl K, Edalati A, Oderup C, Habtezion A, Pachynski R, et al. (2012) Plasmacytoid dendritic cells transport peripheral antigens to the thymus to promote central tolerance. *Immunity* **36**:438-50 https://doi.org/10.1016/j.immuni.2012.01.017 | PubMed

51. **Kim S,** Elkon KB, Ma X (2004) Transcriptional suppression of interleukin-12 gene expression following phagocytosis of apoptotic cells. *Immunity* **21**:643-53 https://doi.org/10.1016/j.immuni.2004.09.009 | PubMed

52. **Chung EY,** Kim SJ, Ma XJ (2006) Regulation of cytokine production during phagocytosis of apoptotic cells. *Cell Res* **16**:154-61 https://doi.org/10.1038/sj.cr.7310021 | PubMed

53. **Huynh MLN,** Fadok VA, Henson PM (2002) Phosphatidylserine-dependent ingestion of apoptotic cells promotes TGF-β1 secretion and the resolution of inflammation. *J Clin Invest* **109**:41 https://doi.org/10.1172/jci11638 | PubMed

54. **de Pooter RF,** Cho SK, Carlyle JR, Zúñiga-Pflücker JC (2003) In vitro generation of T lymphocytes from embryonic stem cell–derived prehematopoietic progenitors. *Blood* **102**:1649-53 https://doi.org/10.1182/blood-2003-01-0224 | PubMed

**Wang H,** Zuniga-Pflucker JC (2026) Uncovering the Heterogeneity and Ontogeny of Mouse Thymic Macrophages Reveals an Unexpected Early Checkpoint Role. NCBI Gene Expression Omnibus. ID GSE326594 https://www.ncbi.nlm.nih.gov/geo/query/acc.cgi?acc=GSE326594

**Hamidzada H,** Epelman S (2022) Three tissue resident macrophage subsets co-exist across organs with conserved origins and lifecycles. NCBI Gene Expression Omnibus. ID GSE188647 https://www.ncbi.nlm.nih.gov/geo/query/acc.cgi?acc=GSE188647

**Zhou T,** Dzhagalov IL (2021) Single-cell RNA-sequencing of thymic myeloid cells from Csf1rgfp/gfp (MaFIA) and Cd11cyfp/yfp mice. NCBI Gene Expression Omnibus. ID GSE185460 https://www.ncbi.nlm.nih.gov/geo/query/acc.cgi?acc=GSE185460

# Peer reviews

## Reviewer #1 (Public review):

Summary:

The current manuscript characterizes in detail the macrophages in the thymus. The authors identify two distinct populations of thymic macrophages and describe their surface marker expression and transcriptional signatures. They also explore their ontology and kinetics of settling and persistence in the thymus and find that the TIMD4+ macrophages are derived from embryonic progenitors and self-maintain in the thymus, while the TIMD4- macrophages are derived from monocytes. Most importantly, the authors test the functional importance of thymic macrophages for T cell development using an in vitro depletion system, from which they conclude that macrophages are important for one of the earliest selection steps in T cell development - the beta selection.

Strengths:

The authors use state-of-the-art techniques, such as multiple genetically modified mice, multi-color flow cytometry, single-cell RNA sequencing, genetic fate mapping, and fetal thymic organ culture (FTOC) combined with depletion. Their work is in good agreement with prior published studies on the subject, such as Tacke et al. (PMID: 26091486) and Zhou et al. (PMID: 36449334). In addition to reproducing prior knowledge, the authors uncover novel and unexpected facets of thymic macrophage biology, such as their SpiC independence and the fact that TIMD4- thymic macrophages depend on CCR2 (Tacke et al. have shown that the overall thymic macrophage compartment is normal in CCR2-/- mice). Most surprisingly, the authors claim that thymic macrophages control an early checkpoint in T cell development, the beta selection. This has not been reported before, as beta selection is usually considered a cell-autonomous process in thymocytes that does not require input from other cells.

Weaknesses:

The thymic macrophage depletion experiments are not well controlled, and the authors' interpretation of the results is a stretch. First, the treatment depletes other cell types, most notably dendritic cells (DCs), which have well-known roles in thymic selection (though not specifically in beta selection). The authors' reasoning that macrophages are abundant in the cortex, where beta selection occurs, while DCs are enriched in the medulla, seems questionable, as the embryonic thymus typically lacks (or has very small) medulla. A second salient point is that the authors haven't ruled out direct toxicity of the dimerizer drug AP20187 on thymocytes (specifically DN cells) in MAFIA mice.

Altogether, this is a solid manuscript that largely confirms the previously established ontogeny and heterogeneity of thymic macrophages. However, the participation of thymic macrophages in beta selection needs stronger evidence.

https://doi.org/10.7554/eLife.109219.1.sa1

## Reviewer #2 (Public review):

This manuscript from Zuniga-Pflucker laboratory describes that thymic macrophages are heterogeneous in flow cytometric and transcriptomic profiles, containing two major populations characterized by TIMD4 and CX3CR1 expression. These macrophage populations are both parenchymal in the thymus but are unequal in developmental ontogeny, Flt3 expression history, and CCR2 dependency. The manuscript further reports the interesting findings that the depletion of thymic macrophages impairs thymocyte development at the DN3 beta-selection checkpoint. These results provide an important advance for further understanding of thymus biology, especially in view of the contribution of heterogenous thymic macrophage subpopulations.

However, Zhou et al. previously reported essentially similar heterogeneity in thymic macrophages. It was demonstrated that TIMD4+ macrophages and CX3CR1+ macrophages have distinct origins and are different in developmental characteristics (27). The authors should better clarify what was previously demonstrated and what is newly described in this study. Zhou, et al. also demonstrated that TIMD4+ macrophages are localized in the cortex whereas CX3CR1+ macrophages distribute in the medullary region. Whether or not these previous findings are reproduced and supported in the present study is important in view of the new finding that thymic macrophages are important for beta-selection, which is presumed to occur in the thymic cortex. The authors may be able to suggest more strongly that TIMD4+ macrophages regulate beta-selection in the thymic cortex through phagocytic efferocytosis. (Indeed, the Figure 1 legend states that frozen thymic sections were used for immunofluorescent staining to identify the localization of thymic macrophages, without showing the results.)

https://doi.org/10.7554/eLife.109219.1.sa0